Novel MRI Approaches for Assessing Cerebral Hemodynamics in Ischemic Cerebrovascular Disease

Manus J. Donahue, Megan K. Strother and Jeroen Hendrikse

Stroke. 2012;43:903-915; originally published online February 16, 2012;
doi: 10.1161/STROKEAHA.111.635995
Stroke is published by the American Heart Association, 7272 Greenville Avenue, Dallas, TX 75231

Print ISSN: 0039-2499. Online ISSN: 1524-4628

Novel MRI Approaches for Assessing Cerebral Hemodynamics in Ischemic Cerebrovascular Disease

Manus J. Donahue, PhD; Megan K. Strother, MD; Jeroen Hendrikse, MD, PhD

Abstract—Changes in cerebral hemodynamics underlie a broad spectrum of ischemic cerebrovascular disorders. An ability to accurately and quantitatively measure hemodynamic (cerebral blood flow and cerebral blood volume) and related metabolic (cerebral metabolic rate of oxygen) parameters is important for understanding healthy brain function and comparative dysfunction in ischemia. Although positron emission tomography, single-photon emission tomography, and gadolinium-MRI approaches are common, more recently MRI approaches that do not require exogenous contrast have been introduced with variable sensitivity for hemodynamic parameters. The ability to obtain hemodynamic measurements with these new approaches is particularly appealing in clinical and research scenarios in which follow-up and longitudinal studies are necessary. The purpose of this review is to outline current state-of-the-art MRI methods for measuring cerebral blood flow, cerebral blood volume, and cerebral metabolic rate of oxygen and provide practical tips to avoid imaging pitfalls. MRI studies of cerebrovascular disease performed without exogenous contrast are synopsized in the context of clinical relevance and methodological strengths and limitations. **(*Stroke*. 2012;43:903-915.)**

Key Words: cerebral blood flow ■ cerebral blood volume ■ cerebral hemodynamics ■ stroke ■ stenosis ■ cerebrovascular disease ■ MRI

The aim of this review is to discuss noninvasive (without contrast injection) MRI methods that are available to assess cerebral blood flow (CBF), cerebral blood volume (CBV), cerebral metabolic rate of oxygen ($CMRO_2$), and oxygen extraction fraction (OEF) in the setting of cerebrovascular disease. Many such methods have recently been shown to provide comparable contrasts to more established invasive techniques and have been used with appropriate modifications to characterize tissue-level hemodynamics in patients with acute and chronic ischemia.

Physiologically, as cerebral perfusion pressure (CPP) reduces, the extent of hemodynamic compromise at the tissue level reflects the autoregulatory capacity of vasculature to increase CBV and/or develop collaterals to supplement CBF. CBF collateralization, as well as regional variability in CBV and OEF, have been hypothesized to correlate uniquely with stroke risk, with evidence suggesting that risk positively correlates with elevated CBV and OEF.[1] Detailed measurements of CBF, CBV, OEF, and $CMRO_2$ have provided important clues regarding progression of cerebrovascular disease,[2,3] and accurate measurements of hemodynamic compromise have the potential to improve diagnosis and risk stratification.[1] Yet, hemodynamic measures are not standardized for the acute or long-term assessment of cerebrovascular disease. The critical barrier to achieving this rests with a lack of (1) methodology for measuring tissue hemodynamics with high specificity and availability and (2) noninvasive approaches capable of monitoring longitudinal progression of impairment.

Recently, additional MRI methods have been developed that claim to provide quantitative information of cerebral hemodynamic status, yet in reality have varying degrees of reproducibility and ease of implementation. By combining these techniques with structural scanning, a state-of-the-art MRI protocol could in principle provide both information on the stage of tissue-level disease and the distribution and size of cerebral infarcts. An overview of novel MRI methods is presented, with comparisons to positron emission tomography and single-photon emission tomography (PET and SPECT) in healthy individuals and in patients when available. The precision, availability, expertise, and clinical relevance of these MRI approaches are summarized in the context of cerebrovascular disease.

Received August 12, 2011; accepted November 29, 2011.

From the Department of Radiology (M.J.D., M.K.S.), the Department of Psychiatry (M.J.D.), and the Department of Physics (M.J.D.), Vanderbilt University, Nashville, TN; and the Department of Radiology, University Medical Center Utrecht, The Netherlands (J.H.).

The online-only Data Supplement is available with this article at http://stroke.ahajournals.org/lookup/suppl/doi:10.1161/STROKEAHA.111.635995/-/DC1.

Correspondence to Manus J. Donahue, PhD, Psychiatry, Physics, Radiology and Radiological Sciences, 1161 21st Ave S, MCN, AAA-3115, Nashville, TN 37232–2310. E-mail mj.donahue@vanderbilt.edu

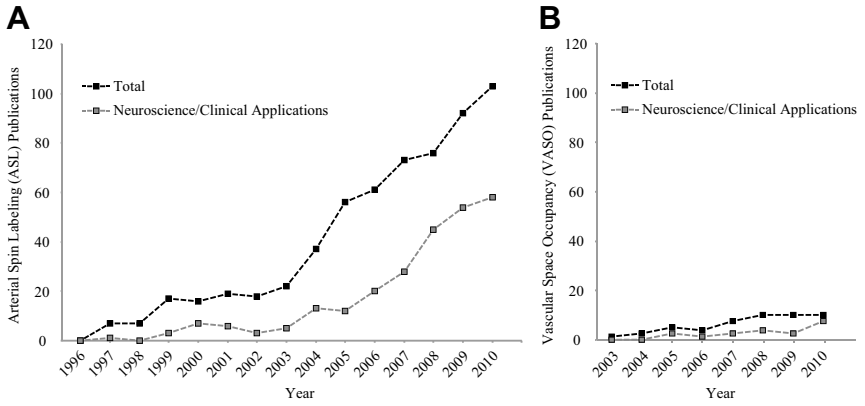

Figure 1. The growing popularity of non-invasive hemodynamic MRI. **A**, Yearly total number of arterial spin labeling (ASL), and **B**, vascular-space-occupancy (VASO) publications since 1996 (ASL) and 2003 (VASO) and corresponding total number of non-methodological studies of these techniques where the focus was specifically to use the method for addressing a neurophysiological question.

Hemodynamic MRI: State of the Field

The gold standard imaging methods to assess hemodynamic impairment have been PET for CBF, CBV, OEF, and $CMRO_2$ and additionally SPECT for measurements of CBF and CBV. Still, PET and SPECT measurements are not often performed in the diagnostic workup of patients, largely owing to difficulty in routine implementation and the exogenous tracers required, which are unavailable in nonspecialized centers. MRI is more widely available and faster than PET and SPECT. Diffusion-weighted imaging (DWI) and fluid-attenuated inversion recovery (FLAIR) MRI sequences are currently the most sensitive methods for identifying small and large acute, subacute, and enduring ischemic infarcts. DWI, which has high diagnostic accuracy and is the gold standard for identifying acute stroke, requires less than 2 minutes of scan time.[4]

Perfusion MRI provides additional information about hemodynamic compromise. The majority of MRI perfusion studies exploit gadolinium (Gd)-dynamic susceptibility contrast (DSC), wherein a Gd chelate is injected intravenously (4–6 mL/s) and tracked by acquiring a 90–120–second time series of single-shot gradient echo images (TR/TE≈1.5/0.03 seconds). Application of tracer kinetics models to the temporal changes in signal permit mean transit-time (MTT), time-to-peak (TTP), CBV, and, to a lesser extent, CBF quantification. Gd-DSC has been used extensively in both chronic and ischemic cerebrovascular disease, and many reviews are available.[5,6] Recent acute stroke trials utilizing Gd-DSC to stratify patients according to perfusion/diffusion mismatch and infarction risk include the Desmoteplase in Acute Ischemic Stroke (DIAS)[7] and DIAS-2 trials,[8] Dose Escalation of Desmoteplase for Acute Ischemic Stroke (DEDAS) trial,[9] and the Diffusion and Perfusion Imaging Evaluation for Understanding Stroke Evolution (DEFUSE) trial.[10]

Ongoing developments in the Gd-DSC field focus on optimization of automated postprocessing routines and related evaluation of algorithms capable of predicting tissue fate during and after ischemia. Although no software combination is capable of reliably predicting tissue fate in all scenarios, novel CBF thresholding approaches and automated analysis software have shown promise for predicting differential responses to reperfusion[11] and identifying lower-boundaries of brain tissue progressing to infarction.[12]

However, Gd-DSC requires the injection of a contrast agent, which, over the past decade, has been dose-restricted because of its association with nephrogenic systemic fibrosis.[13] In clinical populations in which Gd-based contrast agents are contraindicated, such as patients with renal insufficiency, Gd-DSC is generally not permitted for research purposes. Dose restrictions also limit the use of Gd-DSC in longitudinal protocols in which multiple, repeated measurements may be desired. Therefore, research studies are increasingly using new approaches that do not require Gd-based contrast agents.

New MRI Approaches for Assessing CBF

Arterial spin labeling (ASL) MRI[14] is currently the most popular MRI method for measuring CBF that does not require exogenous contrast, and ASL is being implemented in an increasing number of methodological and clinical studies (Figure 1). In ASL, radiofrequency pulses are applied to the blood water proximal to tissue. A delay time is allowed (1.5–2 seconds) whereby the radiofrequency-labeled blood water protons travel to the brain tissue and exchange with tissue water. Consequently, a small reduction occurs in the tissue water magnetization, which is proportional to the amount of exchange, or CBF. However, the change in magnetization when the labeling pulse is applied is very small relative to the total amount of signal. Thus, images acquired during labeling are subtracted from a control (unlabeled) image. Models of tracer kinetics[15] are then applied to the ASL difference signal to quantify CBF in absolute units of mL blood/100 g tissue per minute.

The principles of ASL are analogous to those of $H_2{}^{15}O$ PET CBF measurements,[16] because both are fundamentally freely diffusible tracer-based approaches. However, whereas the tracer in PET is injected $H_2{}^{15}O$, the tracer in ASL is endogenous blood water. For PET, the half-life of ^{15}O is approximately 2 minutes, whereas the blood water tracer in ASL will decay more quickly, with the longitudinal relaxation time, or T_1, of blood water. At 1.5 T, this value is quite short (≈1.2 seconds); however at 3.0 T and 7.0 T, this increases to approximately 1.7 and 2.5 seconds, respectively.[17] The relatively fast decay of the endogenous tracer in ASL allows for repeated measurements to be obtained in a

Table 1. Hemodynamic Methods Comparison

Citation	First Author	Year	MRI Technique (Parameter)	Reference Technique (Parameter)	Population	n	Findings
19	Noguchi	2011	ASL (CBF)	SPECT (CBF)	Moyamoya	12	Hemispherical CBF correlated between ASL and SPECT
20	Liu	2011	ASL (CBF)	SPECT (CBF)	Gulf war illness	47	CBF trends similar between ASL and SPECT (SPECT data from separate study)
21	Uh	2011	VASO (CBV)	PET (CBV)	Controls	8	CBV similarity between VASO and PET
22	Donahue	2010	iVASO (CBV)	Gd-DSC	ICA steno-occlusion	17	CBV correlation between iVASO and Gd-DSC
23	Wissmeyer	2010	ASL (CBF)	PET (CBF)	Epilepsy	3	CBF correlation between ASL and PET
24	Xu	2010	ASL (CBF)	PET (CBF)	Elderly controls	9	Global and regional CBF agreement between ASL and PET
25	Qiu	2010	ASL (CBF)	PET (CBF)	Controls	14	Variations in AAT influence regional ASL CBF quantification
26	Bokkers	2010	ASL (CBF)	PET (CBF)	ICA occlusion	14	CBF overestimation in ASL relative to PET
27	Knutsson	2010	ASL (CBF)	Gd-DSC	Brain tumor	15	Linear correspondence between ASL and Gd-DSC
28	Lüdemann	2009	ASL (CBF)	PET (CBF)	Glioma	12	CBF measured most reliably with ASL compared to other methods
29	Chen	2008	ASL (CBF)	PET (CBF)	Controls	10	CBF correlation between ASL and PET; ASL yielded slightly lower CBF
30	Newberg	2005	ASL (CBF)	PET (CMR_{Glc})	Controls	5	Concordance between ASL CBF and PET-measured cerebral metabolic rate of glucose
31	Kimura	2005	ASL (CBF)	PET (CBF)	ICA occlusion	11	ASL and PET correlation; ASL CBF underestimation ipsilateral to the carotid occlusion
32	Wintermark	2005	ASL (CBF)	PET, SPECT, Gd-DSC	Multiple	. . .	Review of perfusion imaging techniques
33	Weber	2003	ASL (CBF)	Gd-DSC	Brain metastases	62	Comparable CBF contrast in healthy tissue found using ASL and Gd-DSC
34	Liu	2001	ASL (CBF)	PET (CBF)	Epilepsy	8	Correlation between ASL and PET hypoperfusion
35	Ye	2000	ASL (CBF)	PET (CBF)	Control subjects	12	Gray matter CBF similar between ASL and PET; white matter CBF underestimated with ASL

ASL indicates arterial spin labeling; CBF, cerebral blood flow; SPECT, single-photon computed tomography; VASO, vascular-space-occupancy; PET, positron emission tomography; CBV, cerebral blood volume; ICA, internal carotid artery; Gd-DSC, gadolinium–dynamic susceptibility contrast.

short time period (4–8 seconds) and even for changes in CBF in response to neuronal or vascular tasks to be assessed.[18] Cross-modality comparisons (Table 1) have been performed, which generally report comparable CBF contrast between ASL, PET, SPECT, and DSC.

There are a variety of ASL approaches that differ regarding how the labeling is applied[36] and can be grouped into two categories: pulsed ASL (PASL) and continuous ASL (CASL). The difference between PASL and CASL is the labeling scheme for PASL occurs using one[37] or two[38] radiofrequency pulses of duration 3–15 ms, which label blood water over a large volume (80–120 mm) in the neck. Conversely, a long labeling pulse (1.5–2 seconds) is applied in CASL at a single location in the neck.[39,40] The signal-to-noise ratio (SNR) achieved with CASL is 30–50% higher relative to PASL methods,[41] and therefore in

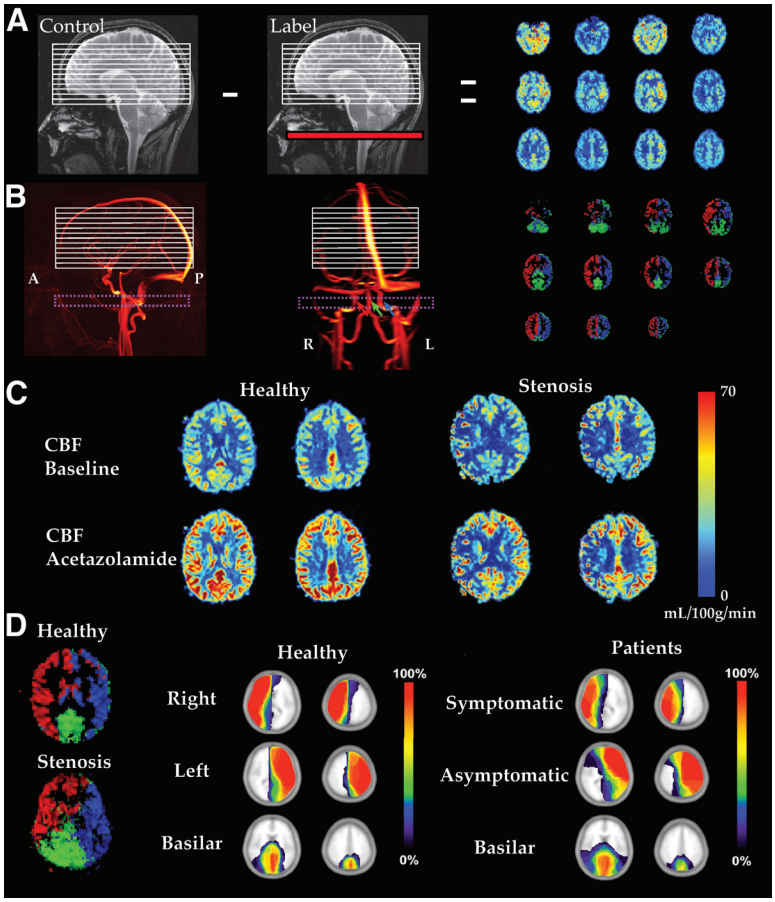

Figure 2. Cerebral blood flow (CBF) imaging using arterial spin labeling (ASL) MRI. **A**, Pseudocontinuous ASL (pCASL) approach in which CBF-weighted maps are obtained from subtraction of a labeled (red) blood water acquisition from an unlabeled control acquisition. **B**, Vessel-selective ASL in which blood water is separately labeled in right internal carotid artery (ICA) (red), left ICA (blue), and basilar (green) arteries; **right**, corresponding CBF maps are generated. **C**, Example baseline and acetazolamide pCASL-CBF maps for a healthy volunteer and a patient with symptomatic right ICA stenosis. **D**, Vessel-selective pCASL shows altered posterior and right flow territories in a patient with right ICA stenosis. **Right**, Axial flow-territory maps projected on a standardized atlas for healthy control participants (n=20) and patients with symptomatic ICA stenosis (n=23). Scale indicates percentage of individuals in the denoted group with measured perfusion.

principle CASL is most desirable. However, historically, the PASL method was used because the short pulses could readily be played out with standard MRI body coils, whereas the longer pulse in the CASL sequence required specialized, local transmit coils.[42]

CBF measurements with PASL MRI depend on the distance between the labeling and imaging region[43] which varies spatially across the brain. For instance, borderzone or watershed areas supplied by end branches of feeding arteries may have increased arterial arrival time (AAT), or time required for blood water to move from the tagging plane to the capillary exchange site. The AAT is generally on the order of 500–1100 ms[44,45] but may be longer in patients with arterial occlusion and collateral flow.[46,47] The long AAT may result in an underestimation of CBF when blood water does not reach the tissue. In patients with intracranial atherosclerotic stenosis or Moyamoya configuration, ASL also may overestimate CBF in focal spots close to the vasculature due to increased endovascular signal caused by prolonged AATs. To address this, PASL data may be acquired at multiple postlabeling delay times, generally 300–2500 ms, which allows for simultaneous quantification of AAT and CBF. The feasibility of this approach has been demonstrated in steno-occlusive disease[46,48] and validated against SPECT.[25,27,25] However, ASL obtained at multiple labeling delays generally requires additional scan time relative to single-delay approaches. Whole-brain coverage with a single postlabeling delay can be obtained in 2–4 minutes, whereas multidelay approaches with comparable resolution require 5–8 minutes. Although the rapid decay of signal creates challenges for ASL tracer labeling, the signal decay is critical for measuring changes in CBF in response to neuronal or vascular tasks,[18] information that cannot be gleaned from Gd-DSC, PET, or SPECT.

A recent ASL improvement is pseudocontinuous ASL (pCASL).[41] In pCASL (Figure 2), labeling is performed over a long duration, as with CASL, but with a series of shorter pulses. These shorter pulses can be applied with available body coils and provide SNR improvements comparable to CASL.[41] pCASL methods have recently increased in popularity, and pCASL probably will be the ASL method of choice in hospital MRI exams. pCASL largely preserves the higher SNR of CASL and is less sensitive to AAT than PASL.

ASL is most robust when used to measure regions of decreased CBF in the cerebral cortex, which can be clearly distinguished from the surrounding areas of normal CBF. Alternatively, white matter CBF is 2–3 times lower than gray matter, and combined with the longer white matter AAT (≈1.5–2.5 seconds), the ASL signal in the white matter is typically just above the background noise level,[49] making it difficult to detect hypoperfused white matter. Challenges caused by delayed AAT may be offset by a recent innovation called velocity-selective ASL. In this technique, arterial blood that decelerates can be labeled in close proximity to the brain tissue, thereby reducing signal loss from delayed AAT.[50]

A rapidly emerging labeling strategy is vessel-selective ASL (VS-ASL). In VS-ASL, different feeding arteries (commonly left and right internal carotid arteries and basilar artery) are separately labeled, thereby giving a measure of perfusion territories and collateralization.[51,52] This approach (Figure 2) has been the target of much recent development work and has been successfully applied in patients with cerebrovascular disease to assess compensatory flow patterns.[53]

Several technical improvements to the ASL sequences complement the labeling strategies mentioned above. Background suppression, which reduces the static gray and white matter signal, improves SNR in most ASL variants.[54,55] Also, "crusher" gradients can be applied in ASL acquisitions to suppress arterial signal in large vessels, allowing for improved CBF contrast without contamination from intravascular blood water. Different imaging readout options are available as well. The most popular readout is single-shot (2D) echo planar imaging (EPI), but it has been difficult to obtain whole-brain coverage using 2D readouts. The multiple excitation pulses required result in slice-dependent labeling delays, complicating CBF quantification. Three-dimensional GRadient and Spin Echo (GRASE) readouts have been applied to remove this slice-timing discrepancy.[56] Compared with 2D EPI readouts, 3D GRASE readouts have shown a 200–300% increase in SNR.[56] ASL with 3D-GRASE has been applied to investigate baseline,[57,58] pharmacological,[59] and neurovascular coupling[18] phenomena in healthy volunteers as well as CBF modulations in patients with steno-occlusive carotid artery disease.[46]

ASL has been used to assess CBF variation in cerebrovascular disease in many human studies (Table 2). Improvements in the past decade allow ASL to be applied clinically to obtain reliable measurements of whole-brain CBF at a field strength of 3.0 T. Many of the more successful clinical ASL studies have been performed at 3.0 T rather than 1.5 T. This is both due to the longer blood water T_1 at 3.0 T (longer label duration) and the SNR increase at 3.0 T.

pCASL approaches with background suppression and flow-crushing gradients in conjunction with 2D or 3D readouts provide CBF values comparable to PET and SPECT. However, unlike PET and SPECT, these measurements can be obtained in 3 to 5 minutes, at a higher spatial resolution of 3 to 5 mm (isotropic voxel dimensions), and with VS-ASL, which together result in less partial volume effects in the cortical ribbon and smaller subcortical structures and additional information regarding collateral flow behavior.

Cerebral Blood Volume

Total CBV quantification in humans is possible with the use of invasive contrast agents and Gd-DSC,[96] PET,[97] CT,[98] and SPECT.[99] MRI approaches using endogenous contrast for measuring total and venous CBV response to neuronal stimulation have been proposed and ASL MRI approaches are being modified to allow for estimation.[100,101] Such approaches can provide reproducible and comparable results to contrast agent-based techniques and have promise for clinical imaging of steno-occlusive disease.

More specifically, vascular-space-occupancy (VASO) MRI has been used to noninvasively measure CBV adjustments associated with increased neuronal activity.[102] In VASO, blood water signal is nulled and the resulting image contains signal primarily from extravascular tissue. Reductions in the measured tissue signal are then used to quantify increases in the vascular compartment volume that accompany neuronal activity. The VASO contrast mechanism has been investigated and information regarding signal changes,[103–105] CSF contamination,[104,105] consistency with other CBV-weighted approaches,[106] blood inflow and T_1 variation,[107] and clinical feasibility (Table 2) have been investigated. Although VASO is much less popular than ASL (first published in 2003; Figure 1), it has demonstrated a similar increase in popularity as ASL over the same postdiscovery time frame. Validation studies have been performed comparing VASO contrast with more established monocrystalline iron oxide nanoparticle (MION)-CBV,[106] PET CBV,[21] and Gd-DSC[22] approaches, reinforcing the CBV sensitivity of VASO. VASO has been applied in a range of neurovascular coupling[108] and functional MRI methodology studies[109–112] as well as in clinical applications of steno-occlusive disease,[22,70] Alzheimer's disease,[113] and cancer.[114,115]

Recently, a modification has been introduced to the VASO sequence in which only blood water below the imaging volume is nulled. This "inflow VASO" (iVASO) approach increases SNR over conventional VASO and is primarily sensitive to arterial CBV (aCBV) adjustments.[116] An additional improvement to iVASO, termed iVASO with dynamic subtraction (iVASO-DS), utilizes the difference between a consecutively acquired control (tissue+blood signal) and null (tissue signal only) image to quantify absolute aCBV.[22] The subtraction procedure is similar to ASL, except instead of tagging the blood water as is done in ASL, blood water signal is nulled by choosing the labeling delay to correspond to the blood water null time; the time needed for blood nulling is approximately on the order of arterial-to-capillary transit times (700–1100 ms), which is why the sensitivity is primarily arterial.

Using iVASO-DS, aCBV values have been reported in-line with expected values from the literature, and between-subject aCBV values vary over a physiologically expected range. Depending on the imaging modality used and region studied, total gray matter CBV is generally reported as 4.7–5.5 mL/100 mL,[117] and healthy precapillary CBV is commonly approximated as 20–30% of total CBV.[118] This would lead to an expected aCBV of 0.94–1.65 mL/100 mL, consistent with iVASO-DS aCBV measures. iVASO-DS has very recently been applied to assess CBV modulations in patients with internal carotid artery steno-occlusive disease (Figure 3) and has been compared with Gd-DSC.[22]

A similar approach that has been proposed for assessment of absolute aCBV is quantitative STAR labeling of arterial regions (QUASAR).[100] Similar to iVASO-DS, aCBV is quantified in QUASAR on subtraction of data

Table 2. Human Baseline and Reactivity Cerebrovascular Disease Studies

Citation	First Author	Year	MRI Technique (Parameter)	Disease	n	Findings
Stroke						
46	MacIntosh	2010	ASL (CBF, AAT)	Acute minor stroke or TIA	30	Reduced CBF and increased AAT in patients relative to controls
60	Chen	2009	ASL (CBF)	Pediatric ischemic stroke	10	Acute and follow-up infarct volumes largest in cases with hypoperfusion
61	Hendrikse*	2009	ASL (CBF)	Ischemia	159	ASL provides diagnostic capability in 92% of patients
62	Zhao*	2009	ASL (CBF)	Chronic middle cerebral artery stroke	87	Despite preserved vasoconstriction, CBF augmentation is inadequate in many vascular territories in patients with large-artery ischemic disease
63	Pollock	2008	ASL (CBF)	Anoxic injury	16	Gray matter CBF significantly higher in anoxic injury subjects
64	Wolf	2003	ASL (CBF)	Acute and/or chronic cerebrovascular disease	10	Invasive CBF measurements correlated with ASL CBF measurements in patients who did not have major transit time delays
65	Chalela	2000	ASL (CBF)	Acute ischemic stroke	15	ASL detects perfusion/diffusion (DWI) mismatches in acute ischemic stroke patients
66	Detre	1998	ASL (CBF)	Stroke, TIA, or severe ICA stenosis	14	Good-quality CBF-weighted maps can be obtained using ASL in patients
ICA disease						
67	Bokkers*	2011	ASL (CBF)	ICA occlusion	32	ASL identified regional impaired acetazolamide-induced cerebrovascular reactivity in patients relative to control subjects
68	Hartkamp	2011	ASL (CBF)	ICA stenosis	53	Caudate nucleus is supplied with blood by the contralateral ICA more frequently in patients than control subjects
69	Bokkers	2010	ASL (CBF)	ICA stenosis	43	Vasodilatory capacity and regional variability in flow territories of major cerebral arteries can be visualized with ASL
26	Bokkers	2010	ASL (CBF)	ICA occlusion	14	ASL at multiple delay times depicts areas of reduced CBF in patients; overestimation of CBF relative to $H_2{}^{15}O$ PET was noted
22	Donahue*	2010	iVASO (arterial CBV)	ICA stenosis or occlusion	25	Arterial CBV elevated in brain hemisphere from which symptoms were derived in 41% of patients; no asymmetry found in control subjects
70	Donahue	2009	VASO (CBV)	ICA stenosis or occlusion	20	Feasibility study demonstrating that CBV-weighted reactivity is altered in patients relative to control subjects
71	Van Laar*	2008	ASL (CBF)	ICA stenosis or occlusion	130	Hypertension is related to higher CBF and hyperhomocysteinemia to lower regional CBF
72	Chng	2008	ASL (CBF)	ECA or ICA stenosis	18	Agreement observed between digital subtraction angiography and territorial ASL for the assessment of collateral flow
73	Haller*	2008	BOLD (CBF, CBV, $CMRO_2$)	ICA stenosis	24	Severely reduced pretreatment CO_2-induced BOLD reactivity was associated with increased occurrence of peri-interventional therapy infarction
74	Mandell	2008	BOLD (CBF, CBV) and ASL (CBF)	ICA stenosis	38	CO_2-induced BOLD reactivity correlates with CO_2-induced CBF-weighted ASL reactivity
75	Van Laar*	2007	ASL (CBF)	ICA stenosis	24	Differences in flow territories and regional CBF between patients and control subjects reduced after carotid angioplasty with stent placement; changes in flow territories and regional CBF were similar in patients who underwent carotid angioplasty with stent placement or carotid endarterectomy
76	Van Laar	2007	ASL (CBF)	ICA occlusion	68	Vessel-selective ASL maps show significant differences in flow territories of the contralateral ICA and vertebrobasilar arteries in patients compared with control subjects
77	Hendrikse	2005	ASL (CBF)	ICA sacrifice	7	Feasibility established for ASL for clinical follow-up of patients after extracranial-intracranial bypass surgery
78	Ziyeh*	2005	BOLD (CBF, CBV, $CMRO_2$)	ICA stenosis or occlusion	27	BOLD reactivity measurements include diagnostic information concerning cerebrovascular reserve
79	Hendrikse*	2004	ASL (CBF)	ICA occlusion	11	Reduced CBF in gray matter of hemisphere ipsilateral to occlusion compared with contralateral hemisphere
80	Ances	2004	ASL (CBF)	ICA stenosis	10	Inverse relationship found between change in CBF after carotid endarterectomy versus baseline CBF within the anterior circulation but not for posterior circulation
81	Detre	1999	ASL (CBF)	ICA and/or middle cerebral artery stenosis	14	Feasibility study demonstrating ability of ASL to identify different patterns of CBF augmentation

(*Continued*)

Table 2. Continued

Citation	First Author	Year	MRI Technique (Parameter)	Disease	n	Findings
Cerebrovascular risk factors						
82	Hajjar*	2010	ASL (CBF)	Hypertension	62	Decrease in CO_2-induced CBF reactivity in hypertensive patients without stroke was comparable to the decrease in CBF reactivity in stroke patients without hypertension
83	Fierstra	2010	BOLD (CBF, CBV, $CMRO_2$)	Vascular steal phenomena	17	Spatial correspondence exists between vascular steal and cortical thinning
84	Hajjar*	2010	ASL (CBF)	Acute stroke	80	Nocturnal dipping of lesser magnitude in systolic and pulse pressure is associated with brain atrophy and worse functional status
85	Pollock*	2009	ASL (CBF)	Hospitalized patients with hypercapnic cerebral hyperperfusion or hypocapnic hypoperfusion	45	Significant positive linear relationship between ASL CBF and partial pressure of CO_2
86	Zaharchuk*	2009	ASL (CBF)	Cerebrovascular disease	139	Approximately half of patients with normal contrast-enhanced CBF imaging have abnormal ASL findings, suggesting ASL provides additional information
87	Wu*	2008	Vessel-encoded ASL (CBF)	ICA and/or middle cerebral artery stenosis	56	ASL detects the presence and origin of collateral flow
88	Van Laar*	2008	ASL (CBF)	Vascular risk factors	121	Increasing levels of tumor necrosis factor-α is significantly associated with higher regional CBF
Intracranial stenosis						
89	Mandell*	2011	BOLD (CBF, CBV, $CMRO_2$)	Intracranial stenosis with EC/IC bypass	25	Preoperative measurement of CO_2-induced BOLD reactivity predicts the hemodynamic effect of extracranial-intracranial bypass
90	Zaharchuk*	2011	ASL (CBF)	Moyamoya	18	ASL predicts the presence and intensity of collateral flow in patients
91	Heyn	2010	BOLD (CBF, CBV, $CMRO_2$)	Moyamoya	11	BOLD CO_2-induced reactivity correlates with modified Suzuki score
Sickle cell disease						
92	O'Gorman	2010	ASL (CBF)	Sickle cell disease	1	ASL demonstrates crossed-cerebellar diaschisis
93	Helton	2009	ASL (CBF)	Sickle cell disease	21	Hydroxyurea may normalize gray matter CBF but not white matter CBF in sickle cell anemia children
94	Van den Tweel	2009	ASL (CBF)	Sickle cell disease	12	No CBF difference observed between sickle cell patients and control subjects, yet more CBF asymmetry observed in patients
95	Oguz*	2003	ASL (CBF)	Sickle cell disease	14	Regional CBF variations observed in normal-appearing regions of structural MRI

ASL indicates arterial spin labeling; CBF, cerebral blood flow; AAT, arterial arrival time; TIA, transient ischemic attack; DWI, diffusion-weighted imaging; ICA, internal carotid artery; BOLD, blood oxygenation level–dependent MRI; CBV, cerebral blood volume; $CMRO_2$, cerebral metabolic rate of oxygen; iVASO, inflow vascular-space-occupancy.

*Selected studies with clinical implications, expanded in online-only Data Supplement Table 1 (http://stroke.ahajournals.org).

with and without blood water signal. However, in QUASAR, transverse blood water magnetization is nulled by bipolar dephasing gradients, whereas in iVASO the longitudinal blood water magnetization is nulled through principles of inversion recovery. QUASAR has been evaluated in a large-scale, interinstitutional validation study[45] and has been shown to provide comparable contrast as SPECT in patients with internal carotid artery stenosis.[48]

Other MRI methods for measuring CBV have been proposed but have been validated and implemented to a lesser extent in humans. Using MRI with modulation of tissue and vessel (MOTIVE) signals in isoflurane-anesthetized rats at 9.4 T, it was estimated that aCBV=1.1±0.5 mL/100 mL in cerebral cortex.[101] The MOTIVE technique separately modulates tissue and blood water signal using magnetization transfer and ASL principles. Additionally, venous refocusing for volume estimation (VERVE) has been proposed as a noninvasive MRI method for assessing venous CBV changes in conjunction with readouts with refocusing pulses with varying intervals.[119] MOTIVE and VERVE provide physiological CBV changes, yet have not been systematically evaluated in clinical populations.

Oxygen Metabolism and Consumption

OEF and $CMRO_2$ are important parameters in gauging hemodynamic and metabolic impairment. Despite a large variation in CBF and $CMRO_2$ over the brain, OEF remains relatively constant in healthy individuals. This appears to be true even in early stages of hemodynamic impairment, in which OEF is maintained through regional modulations of CBF and CBV.[1] In acute stroke, CBF and $CMRO_2$ falling below threshold generally indicate irreversible tissue damage. However, preservation of $CMRO_2$ in the face of reduced CBF and increased OEF, or misery perfusion, may indicate viable tissue.

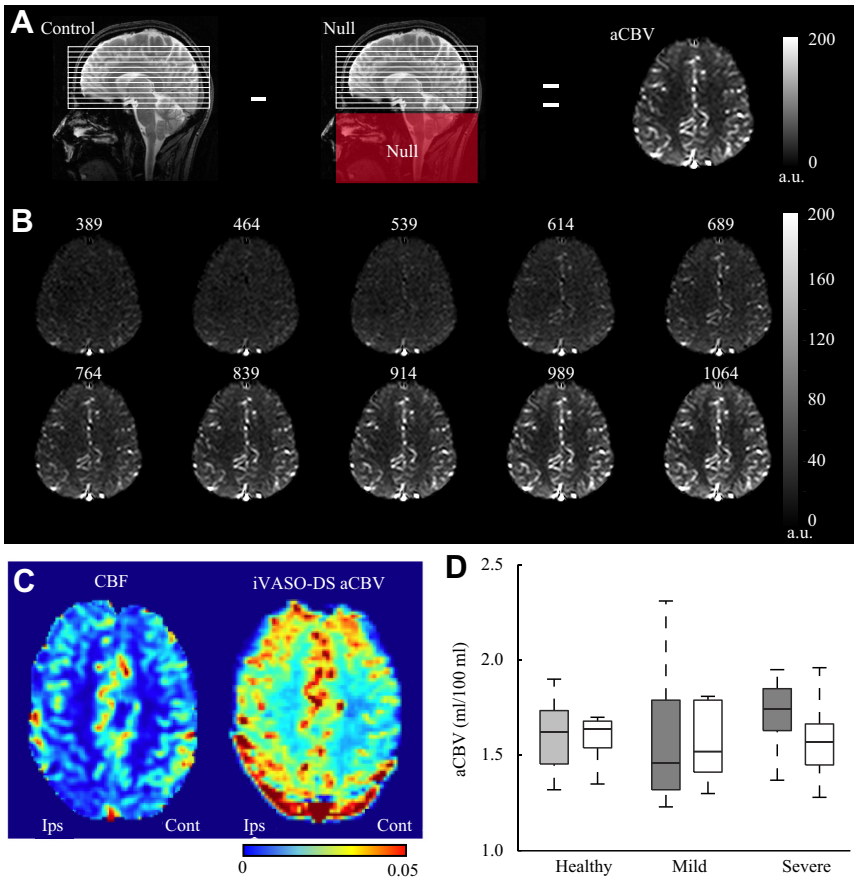

Figure 3. Noninvasive arterial cerebral blood volume (aCBV)-weighted vascular-space-occupancy with dynamic subtraction–dynamic subtraction (iVASO-DS) MRI. **A**, In iVASO-DS, the difference between images with and without inflowing blood water signal yields an aCBV-weighted map. **B**, Such images can be acquired at different labeling delays while keeping the blood water nulled in the null acquisitions, thereby yielding maps of inflowing microvascular aCBV as a function of time (ms; **above**). **C**, Axial slices from a patient with 70% right internal carotid artery (ICA) stenosis. **Left**, CBF-weighted slice from gadolinium–dynamic susceptibility contrast, and **right**, iVASO-DS aCBV map. CBF is symmetrical, yet aCBV is increased in the right parietal lobe, consistent with autoregulation. **D**, Box plots from patients (n=17) with varying degrees of ICA stenosis (mild, 15%≤ICA stenosis <70%; severe, ≥70% ICA stenosis). aCBV was asymmetrically elevated in 41% of patients studied (dark gray is ipsilateral to maximum stenosis).

Like CBF, OEF measurements are possible with the use of PET in conjunction with $H_2{}^{15}O$. Efforts have been made using MRI approaches to similarly measure OEF; however, such approaches are still very much in development. An obvious place to begin is with blood oxygenation level–dependent (BOLD) MRI, which has emerged as the most popular method for assessing brain function.[120] Briefly, BOLD contrast arises owing to a disproportionate increase in CBF relative to CBV and $CMRO_2$ during elevated neuronal or vascular activity,[118] leading to an increase in the oxygenation level of blood in capillaries and veins and corresponding $T_2{}^{(*)}$-lengthening (BOLD effect). BOLD MRI has been widely used as it can easily be implemented with reasonably high spatial (3–4 mm isotropic voxel dimensions) and temporal (2–3 seconds) resolution. Additionally, the most commonly implemented BOLD variant is fundamentally a standard gradient echo sequence, available on any MRI scanner.

Unfortunately, the BOLD effect is only an indirect marker of neuronal activity, and relating the measured response quantitatively to CBF, CBV, $CMRO_2$, and OEF is an area of active research. Much of this effort focuses on measuring CBF, CBV, and OEF changes concurrent to a neuronal or vascular stimulus[18] (Figure 4). Clinically, such an approach has provided promising qualitative results in patients with chronic cerebrovascular disease[74,91] but is not widely applicable in acute settings because impairment frequently precludes task compliance. Thus, recent work has focused on extracting quantitative OEF measurements from baseline images. Feasibility has been demonstrated for applying models to baseline BOLD signal to quantify OEF. This was first suggested in 2000 and later revisited in 2007 on application of a more elaborate multicompartment model.[121,122] This approach has been shown to provide physiological OEF values in healthy volunteers, and in acute stroke patients this method was used to characterize the OEF around the area of ischemic infarcts,[123] yet the approach has not gained clinical attention largely owing to difficulty in the elaborate modeling and quantification assumptions.

More recently, a method for measuring whole-brain OEF has been proposed called T_2-relaxation-under-spin-tagging (TRUST).[124] In this approach, venous T_2 is measured in the sagittal sinus, after which oxygenation level is assigned based on known relationships between blood water T_2 and oxygenation level. This approach has shown potential for measuring whole-brain OEF and for explaining variations in intersubject BOLD variations[125] but does not measure regional variations in OEF. An adaptation of the TRUST approach has been proposed whereby venous oxygenation is targeted more locally using venous blood water labeling in conjunction with velocity selective ASL principles. This approach[126] may be more sensitive to regional variations in OEF; however, clinical implementation and cross-modality validation studies have not yet been performed.

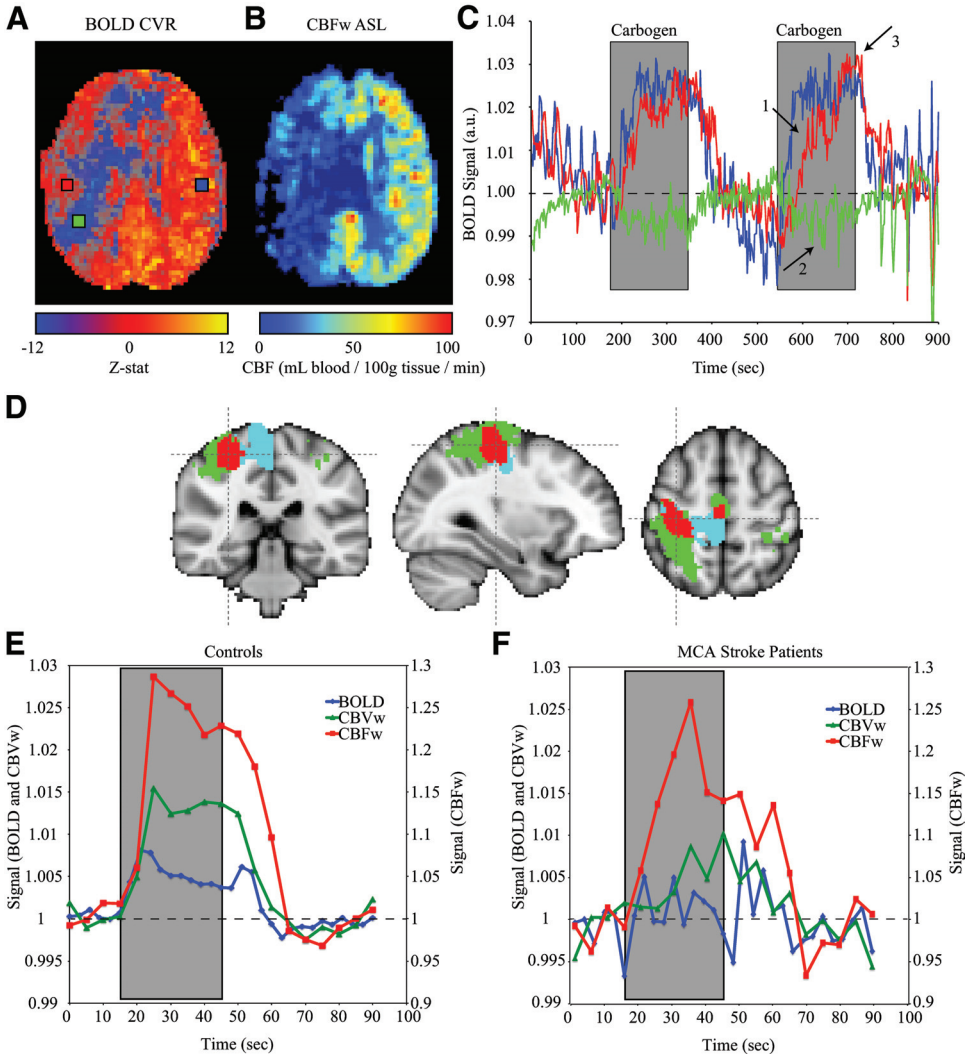

Figure 4. MRI reactivity in cerebrovascular disease. **A**, Moyamoya patient with decreased blood oxygenation level–dependent (BOLD) cerebrovascular reactivity (CVR) in right parietal lobe, and **B**, larger region of compromised cerebral blood flow (CBF) in the right hemisphere on arterial spin labeling (ASL). **C**, BOLD CVR time courses from colored voxels in **A** reveal heterogeneous response to carbogen administration (gray). This includes normal CVR and baseline CBF in the posterior left frontal lobe (blue), delayed CVR with delayed time-to-peak in the right frontal lobe (red; **arrows 1 and 3**), and even negative CVR (green; **arrow 2**), indicative of vascular steal phenomenon in the right parietal lobe. **D** through **F**, Hemodynamic time courses from chronic middle cerebral artery (MCA) stroke patients and controls acquired using BOLD, CBF-weighted ASL, and CBV-weighted vascular-space-occupancy fMRI in sequence. Patients (n=9) with enduring motor impairment were scanned within 1 year after stroke, at which time they performed unilateral joystick movement (f=1 Hz) with their affected hand. **D**, Activation maps (green), anatomic M1 (blue), and common regions (red) for all subjects, normalized to standard space. Time courses in common regions (**D**, red) show robust hemodynamic responses (gray box denotes stimulus period) in control subjects (n=11) but discord in CBF and CBV coupling in patients, eliciting absent ensemble patient BOLD reactivity.

Clinical Implications and Conclusions

We have outlined the state of new MRI approaches for measuring CBF, CBV, $CMRO_2$, and OEF in cerebrovascular disease. The majority of studies using these approaches have occurred in the setting of chronic cerebrovascular disease, with far less work being focused on acute stroke imaging. The primary reason for this is the time required for scanning (approximately 5 minutes per approach) and the image processing required, which has generally not been optimized for acute time demands. However, as these methods become more standardized, it is anticipated that a demand for efficient and fast processing will grow and analysis packages will translate to scanner consoles to facilitate time-sensitive imaging. In general, CBF-weighted ASL approaches have undergone the most advanced clinical testing and have been cross-validated with Gd-DSC, PET and SPECT (Table 1) and extensively applied in cerebrovascular disease (Table 2). Using standard hardware widely available on MRI scanners, pCASL approaches can be applied in less than 5 minutes with spatial resolution of 3 to 4 mm isotropic and whole-brain coverage, making them a reasonable substitute for Gd-DSC. A postlabeling delay of 1.5—2 seconds is generally used, with a longer delay time or multiple delay time protocol (5–8 minutes) required for ischemic patients with delayed AAT. Importantly, and unlike other

methods such as PET, SPECT, and Gd-DSC, ASL can be modified to allow for labeling of blood water in different vessels, thereby providing an image of both CBF and collateral flow (eg, the extent to which CBF is supplied from different feeding vessels). Noninvasive CBV approaches are less advanced than CBF applications, with only VASO and QUASAR applied to human chronic cerebrovascular disease studies. These methods may be useful in patient populations that exhibit abnormal CBF and CBV coupling, whereby when used in sequence with ASL can provide quantitative information regarding both collateral flow and autoregulation. MRI methods for measuring OEF and $CMRO_2$ remain in development, with several promising research applications yet extremely limited clinical assessment. Online-only Data Supplement Table 1 (http://stroke.ahajournals.org) provides more detailed explanations of the direct clinical relevance of some of the most influential studies that have exploited contrast from these approaches.

Sources of Funding

Dr Hendrikse receives support from The Netherlands Heart Foundation (grant-2010B274).

Disclosures

None.

References

1. Derdeyn CP, Videen TO, Yundt KD, Fritsch SM, Carpenter DA, Grubb RL, et al. Variability of cerebral blood volume and oxygen extraction: stages of cerebral haemodynamic impairment revisited. *Brain*. 2002; 125:595–607.
2. Zipfel GJ, Sagar J, Miller JP, Videen TO, Grubb RL Jr, Dacey RG Jr, et al. Cerebral hemodynamics as a predictor of stroke in adult patients with Moyamoya disease: a prospective observational study. *Neurosurg Focus*. 2009;26:E6.
3. Grubb RL Jr, Derdeyn CP, Fritsch SM, Carpenter DA, Yundt KD, Videen TO, et al. Importance of hemodynamic factors in the prognosis of symptomatic carotid occlusion. *JAMA*. 1998;280: 1055–1060.
4. Gonzalez RG, Schaefer PW, Buonanno FS, Schwamm LH, Budzik RF, Rordorf G, et al. Diffusion-weighted MR imaging: diagnostic accuracy in patients imaged within 6 hours of stroke symptom onset. *Radiology*. 1999;210:155–162.
5. Wintermark M, Albers GW, Alexandrov AV, Alger JR, Bammer R, Baron JC, et al. Acute stroke imaging research roadmap. *Stroke*. 2008; 39:1621–1628.
6. Muir KW, Buchan A, von Kummer R, Rother J, Baron JC. Imaging of acute stroke. *Lancet Neurol*. 2006;5:755–768.
7. Hacke W, Albers G, Al-Rawi Y, Bogousslavsky J, Davalos A, Eliasziw M, et al. The desmoteplase in acute ischemic stroke trial (DIAS): a phase II MRI-based 9-hour window acute stroke thrombolysis trial with intravenous desmoteplase. *Stroke*. 2005;36:66–73.
8. Hacke W, Furlan AJ, Al-Rawi Y, Davalos A, Fiebach JB, Gruber F, et al. Intravenous desmoteplase in patients with acute ischaemic stroke selected by MRI perfusion-diffusion weighted imaging or perfusion ct (DIAS-2): a prospective, randomised, double-blind, placebo-controlled study. *Lancet Neurol*. 2009;8:141–150.
9. Furlan AJ, Eyding D, Albers GW, Al-Rawi Y, Lees KR, Rowley HA, et al. Dose escalation of desmoteplase for acute ischemic stroke (DEDAS): evidence of safety and efficacy 3 to 9 hours after stroke onset. *Stroke*. 2006;37:1227–1231.
10. Albers GW, Thijs VN, Wechsler L, Kemp S, Schlaug G, Skalabrin E, et al. Magnetic resonance imaging profiles predict clinical response to early reperfusion: the diffusion and perfusion imaging evaluation for understanding stroke evolution (DEFUSE) study. *Ann Neurol*. 2006;60: 508–517.
11. Lansberg MG, Lee J, Christensen S, Straka M, De Silva DA, Mlynash M, et al. Rapid automated patient selection for reperfusion therapy: a pooled analysis of the echoplanar imaging thrombolytic evaluation trial (EPITHET) and the diffusion and perfusion imaging evaluation for understanding stroke evolution (DEFUSE) study. *Stroke*. 2011;42: 1608–1614.
12. Galinovic I, Ostwaldt AC, Soemmer C, Bros H, Hotter B, Brunecker P, et al. Search for a map and threshold in perfusion MRI to accurately predict tissue fate: a protocol for assessing lesion growth in patients with persistent vessel occlusion. *Cerebrovascular diseases*. 2011;32: 186–193.
13. Jalandhara N, Arora R, Batuman V. Nephrogenic systemic fibrosis and gadolinium-containing radiological contrast agents: an update. *Clin Pharmacol Ther*. 2011;89:920–923.
14. Williams DS, Detre JA, Leigh JS, Koretsky AP. Magnetic resonance imaging of perfusion using spin inversion of arterial water. *Proc Natl Acad Sci U S A*. 1992;89:212–216.
15. Buxton RB, Frank LR, Wong EC, Siewert B, Warach S, Edelman RR. A general kinetic model for quantitative perfusion imaging with arterial spin labeling. *Magn Reson Med*. 1998;40:383–396.
16. Raichle ME. Measurement of local cerebral blood flow and metabolism in man with positron emission tomography. *Fed Proc*. 1981;40: 2331–2334.
17. Rooney WD, Johnson G, Li X, Cohen ER, Kim SG, Ugurbil K, et al. Magnetic field and tissue dependencies of human brain longitudinal 1H2O relaxation in vivo. *Magn Reson Med*. 2007;57:308–318.
18. Donahue MJ, Blicher JU, Ostergaard L, Feinberg DA, MacIntosh BJ, Miller KL, et al. Cerebral blood flow, blood volume, and oxygen metabolism dynamics in human visual and motor cortex as measured by whole-brain multi-modal magnetic resonance imaging. *J Cereb Blood Flow Metab*. 2009;29:1856–1866.
19. Noguchi T, Kawashima M, Irie H, Ootsuka T, Nishihara M, Matsushima T, et al. Arterial spin-labeling MR imaging in Moyamoya disease compared with SPECT imaging. *Eur J Radiol*. 2011;80:e557–e562.
20. Liu P, Aslan S, Li X, Buhner DM, Spence JS, Briggs RW, et al. Perfusion deficit to cholinergic challenge in veterans with Gulf War illness. *Neurotoxicology*. 2011;32:242–246.
21. Uh J, Lin AL, Lee K, Liu P, Fox P, Lu H. Validation of VASO cerebral blood volume measurement with positron emission tomography. *Magn Reson Med*. 2011;65:744–749.
22. Donahue MJ, Sideso E, MacIntosh BJ, Kennedy J, Handa A, Jezzard P. Absolute arterial cerebral blood volume quantification using inflow vascular-space-occupancy with dynamic subtraction magnetic resonance imaging. *J Cereb Blood Flow Metab*. 2010;30:1329–1342.
23. Wissmeyer M, Altrichter S, Pereira VM, Viallon M, Federspiel A, Seeck M, et al. Arterial spin-labeling MRI perfusion in tuberous sclerosis: correlation with PET. *J Neuroradiol*. 2010;37:127–130.
24. Xu G, Rowley HA, Wu G, Alsop DC, Shankaranarayanan A, Dowling M, et al. Reliability and precision of pseudo-continuous arterial spin labeling perfusion MRI on 3.0 T and comparison with 15O-water pet in elderly subjects at risk for Alzheimer's disease. *NMR Biomed*. 2010;23: 286–293.
25. Qiu M, Paul Maguire R, Arora J, Planeta-Wilson B, Weinzimmer D, Wang J, et al. Arterial transit time effects in pulsed arterial spin labeling CBF mapping: insight from a PET and MR study in normal human subjects. *Magn Reson Med*. 2010;63:374–384.
26. Bokkers RP, Bremmer JP, van Berckel BN, Lammertsma AA, Hendrikse J, Pluim JP, et al. Arterial spin labeling perfusion MRI at multiple delay times: a correlative study with H(2)(15)O positron emission tomography in patients with symptomatic carotid artery occlusion. *J Cereb Blood Flow Metab*. 2010;30:222–229.
27. Knutsson L, van Westen D, Petersen ET, Bloch KM, Holtas S, Stahlberg F, et al. Absolute quantification of cerebral blood flow: correlation between dynamic susceptibility contrast MRI and model-free arterial spin labeling. *Magn Reson Imaging*. 2009;28:1–7.
28. Ludemann L, Warmuth C, Plotkin M, Forschler A, Gutberlet M, Wust P, et al. Brain tumor perfusion: comparison of dynamic contrast enhanced magnetic resonance imaging using T1, T2, and T2* contrast, pulsed arterial spin labeling, and H2(15)O positron emission tomography. *Eur J Radiol*. 2009;70:465–474.
29. Chen JJ, Wieckowska M, Meyer E, Pike GB. Cerebral blood flow measurement using fMRI and PET: a cross-validation study. *Int J Biomed Imaging*. 2008;2008:516359.
30. Newberg AB, Wang J, Rao H, Swanson RL, Wintering N, Karp JS, et al. Concurrent CBF and CMRGLC changes during human brain acti-

vation by combined fMRI-pet scanning. *Neuroimage*. 2005;28:500–506.
31. Kimura H, Kado H, Koshimoto Y, Tsuchida T, Yonekura Y, Itoh H. Multislice continuous arterial spin-labeled perfusion MRI in patients with chronic occlusive cerebrovascular disease: a correlative study with CO_2 PET validation. *J Magn Reson Imaging*. 2005;22:189–198.
32. Wintermark M, Sesay M, Barbier E, Borbely K, Dillon WP, Eastwood JD, et al. Comparative overview of brain perfusion imaging techniques. *J Neuroradiol*. 2005;32:294–314.
33. Weber MA, Gunther M, Lichy MP, Delorme S, Bongers A, Thilmann C, et al. Comparison of arterial spin-labeling techniques and dynamic susceptibility-weighted contrast-enhanced MRI in perfusion imaging of normal brain tissue. *Invest Radiol*. 2003;38:712–718.
34. Liu HL, Kochunov P, Hou J, Pu Y, Mahankali S, Feng CM, et al. Perfusion-weighted imaging of interictal hypoperfusion in temporal lobe epilepsy using fair-haste: comparison with H(2)(15)O PET measurements. *Magn Reson Med*. 2001;45:431–435.
35. Ye FQ, Berman KF, Ellmore T, Esposito G, van Horn JD, Yang Y, et al. H(2)(15)O PET validation of steady-state arterial spin tagging cerebral blood flow measurements in humans. *Magn Reson Med*. 2000;44:450–456.
36. Golay X, Hendrikse J, Lim TC. Perfusion imaging using arterial spin labeling. *Top Magn Reson Imaging*. 2004;15:10–27.
37. Kim SG. Quantification of relative cerebral blood flow change by flow-sensitive alternating inversion recovery (fair) technique: application to functional mapping. *Magn Reson Med*. 1995;34:293–301.
38. Golay X, Stuber M, Pruessmann KP, Meier D, Boesiger P. Transfer insensitive labeling technique (TILT): application to multislice functional perfusion imaging. *J Magn Reson Imaging*. 1999;9:454–461.
39. Wong EC, Buxton RB, Frank LR. A theoretical and experimental comparison of continuous and pulsed arterial spin labeling techniques for quantitative perfusion imaging. *Magn Reson Med*. 1998;40:348–355.
40. Alsop DC, Detre JA. Multisection cerebral blood flow MR imaging with continuous arterial spin labeling. *Radiology*. 1998;208:410–416.
41. Wu WC, Fernandez-Seara M, Detre JA, Wehrli FW, Wang J. A theoretical and experimental investigation of the tagging efficiency of pseudocontinuous arterial spin labeling. *Magn Reson Med*. 2007;58:1020–1027.
42. Alsop DC, Connick TJ, Mizsei G. A spiral volume coil for improved RF field homogeneity at high static magnetic field strength. *Magn Reson Med*. 1998;40:49–54.
43. Gonzalez-At JB, Alsop DC, Detre JA. Cerebral perfusion and arterial transit time changes during task activation determined with continuous arterial spin labeling. *Magn Reson Med*. 2000;43:739–746.
44. MacIntosh BJ, Filippini N, Chappell MA, Woolrich MW, Mackay CE, Jezzard P. Assessment of arterial arrival times derived from multiple inversion time pulsed arterial spin labeling MRI. *Magn Reson Med*. 2010;63:641–647.
45. Petersen ET, Mouridsen K, Golay X. The quasar reproducibility study, part II: results from a multi-center arterial spin labeling test-retest study. *Neuroimage*. 2010;49:104–113.
46. MacIntosh BJ, Lindsay AC, Kylintireas I, Kuker W, Gunther M, Robson MD, et al. Multiple inflow pulsed arterial spin-labeling reveals delays in the arterial arrival time in minor stroke and transient ischemic attack. *Am J Neuroradiol*. 2010;31:1892–1894.
47. Bokkers RP, van der Worp HB, Mali WP, Hendrikse J. Noninvasive MR imaging of cerebral perfusion in patients with a carotid artery stenosis. *Neurology*. 2009;73:869–875.
48. Uchihashi Y, Hosoda K, Zimine I, Fujita A, Fujii M, Sugimura K, et al. Clinical application of arterial spin-labeling MR imaging in patients with carotid stenosis: quantitative comparative study with single-photon emission CT. *Am J Neuroradiol*. 2011 [Epub ahead of print].
49. van Osch MJ, Teeuwisse WM, van Walderveen MA, Hendrikse J, Kies DA, van Buchem MA. Can arterial spin labeling detect white matter perfusion signal? *Magn Reson Med*. 2009;62:165–173.
50. Wong EC, Cronin M, Wu WC, Inglis B, Frank LR, Liu TT. Velocity-selective arterial spin labeling. *Magn Reson Med*. 2006;55:1334–1341.
51. Hendrikse J, van der Grond J, Lu H, van Zijl PC, Golay X. Flow territory mapping of the cerebral arteries with regional perfusion MRI. *Stroke*. 2004;35:882–887.
52. Wong EC. Vessel-encoded arterial spin-labeling using pseudocontinuous tagging. *Magn Reson Med*. 2007;58:1086–1091.
53. Bokkers RP, van Osch MJ, Klijn CJ, Kappelle LJ, Hendrikse J. Cerebrovascular reactivity within perfusion territories in patients with an internal carotid artery occlusion. *J Neurol Neurosurg Psychiatry*. 2011 [Epub ahead of print].
54. Garcia DM, Duhamel G, Alsop DC. Efficiency of inversion pulses for background suppressed arterial spin labeling. *Magn Reson Med*. 2005;54:366–372.
55. Ye FQ, Frank JA, Weinberger DR, McLaughlin AC. Noise reduction in 3D perfusion imaging by attenuating the static signal in arterial spin tagging (ASSIST). *Magn Reson Med*. 2000;44:92–100.
56. Gunther M, Oshio K, Feinberg DA. Single-shot 3D imaging techniques improve arterial spin labeling perfusion measurements. *Magn Reson Med*. 2005;54:491–498.
57. Fernandez-Seara MA, Wang Z, Wang J, Rao HY, Guenther M, Feinberg DA, et al. Continuous arterial spin labeling perfusion measurements using single shot 3D Grase at 3 T. *Magn Reson Med*. 2005;54:1241–1247.
58. Filippini N, MacIntosh BJ, Hough MG, Goodwin GM, Frisoni GB, Smith SM, et al. Distinct patterns of brain activity in young carriers of the apoE-epsilon4 allele. *Proc Natl Acad Sci U S A*. 2009;106:7209–7214.
59. MacIntosh BJ, Pattinson KT, Gallichan D, Ahmad I, Miller KL, Feinberg DA, et al. Measuring the effects of remifentanil on cerebral blood flow and arterial arrival time using 3D Grase MRI with pulsed arterial spin labelling. *J Cereb Blood Flow Metab*. 2008;28:1514–1522.
60. Chen J, Licht DJ, Smith SE, Agner SC, Mason S, Wang S, et al. Arterial spin labeling perfusion MRI in pediatric arterial ischemic stroke: initial experiences. *J Magn Reson Imaging*. 2009;29:282–290.
61. Hendrikse J, Petersen ET, Cheze A, Chng SM, Venketasubramanian N, Golay X. Relation between cerebral perfusion territories and location of cerebral infarcts. *Stroke*. 2009;40:1617–1622.
62. Zhao P, Alsop DC, Abduljalil A, Selim M, Lipsitz L, Novak P, et al. Vasoreactivity and peri-infarct hyperintensities in stroke. *Neurology*. 2009;72:643–649.
63. Pollock JM, Whitlow CT, Deibler AR, Tan H, Burdette JH, Kraft RA, et al. Anoxic injury-associated cerebral hyperperfusion identified with arterial spin-labeled MR imaging. *Am J Neuroradiol*. 2008;29:1302–1307.
64. Wolf RL, Alsop DC, McGarvey ML, Maldjian JA, Wang J, Detre JA. Susceptibility contrast and arterial spin labeled perfusion MRI in cerebrovascular disease. *J Neuroimaging*. 2003;13:17–27.
65. Chalela JA, Alsop DC, Gonzalez-Atavales JB, Maldjian JA, Kasner SE, Detre JA. Magnetic resonance perfusion imaging in acute ischemic stroke using continuous arterial spin labeling. *Stroke*. 2000;31:680–687.
66. Detre JA, Alsop DC, Vives LR, Maccotta L, Teener JW, Raps EC. Noninvasive MRI evaluation of cerebral blood flow in cerebrovascular disease. *Neurology*. 1998;50:633–641.
67. Bokkers RP, Wessels FJ, van der Worp HB, Zwanenburg JJ, Mali WP, Hendrikse J. Vasodilatory capacity of the cerebral vasculature in patients with carotid artery stenosis. *Am J Neuroradiol*. 2011;32:1030–1033.
68. Hartkamp NS, Bokkers RP, van der Worp HB, van Osch MJ, Kappelle LJ, Hendrikse J. Distribution of cerebral blood flow in the caudate nucleus, lentiform nucleus and thalamus in patients with carotid artery stenosis. *Eur Radiol*. 2011;21:875–881.
69. Bokkers RP, van Osch MJ, van der Worp HB, de Borst GJ, Mali WP, Hendrikse J. Symptomatic carotid artery stenosis: impairment of cerebral autoregulation measured at the brain tissue level with arterial spin-labeling MR imaging. *Radiology*. 2010;256:201–208.
70. Donahue MJ, van Laar PJ, van Zijl PC, Stevens RD, Hendrikse J. Vascular space occupancy (VASO) cerebral blood volume-weighted MRI identifies hemodynamic impairment in patients with carotid artery disease. *J Magn Reson Imaging*. 2009;29:718–724.
71. van Laar PJ, van Raamt AF, van der Grond J, Mali WP, van der Graaf Y, Hendrikse J. Increasing levels of TNFalpha are associated with increased brain perfusion. *Atherosclerosis*. 2008;196:449–454.
72. Chng SM, Petersen ET, Zimine I, Sitoh YY, Lim CC, Golay X. Territorial arterial spin labeling in the assessment of collateral circulation: comparison with digital subtraction angiography. *Stroke*. 2008;39:3248–3254.

73. Haller S, Bonati LH, Rick J, Klarhofer M, Speck O, Lyrer PA, et al. Reduced cerebrovascular reserve at Co_2 bold MR imaging is associated with increased risk of periinterventional ischemic lesions during carotid endarterectomy or stent placement: preliminary results. *Radiology*. 2008;249:251–258.
74. Mandell DM, Han JS, Poublanc J, Crawley AP, Stainsby JA, Fisher JA, et al. Mapping cerebrovascular reactivity using blood oxygen level-dependent MRI in patients with arterial steno-occlusive disease: comparison with arterial spin labeling MRI. *Stroke*. 2008;39: 2021–2028.
75. Van Laar PJ, Hendrikse J, Mali WP, Moll FL, van der Worp HB, van Osch MJ, et al. Altered flow territories after carotid stenting and carotid endarterectomy. *J Vasc Surg*. 2007;45:1155–1161.
76. van Laar PJ, Hendrikse J, Klijn CJ, Kappelle LJ, van Osch MJ, van der Grond J. Symptomatic carotid artery occlusion: flow territories of major brain-feeding arteries. *Radiology*. 2007;242:526–534.
77. Hendrikse J, van der Zwan A, Ramos LM, van Osch MJ, Golay X, Tulleken CA, et al. Altered flow territories after extracranial-intracranial bypass surgery. *Neurosurgery.* 2005;57:486–494.
78. Ziyeh S, Rick J, Reinhard M, Hetzel A, Mader I, Speck O. Blood oxygen level-dependent MRI of cerebral Co_2 reactivity in severe carotid stenosis and occlusion. *Stroke*. 2005;36:751–756.
79. Hendrikse J, van Osch MJ, Rutgers DR, Bakker CJ, Kappelle LJ, Golay X, et al. Internal carotid artery occlusion assessed at pulsed arterial spin-labeling perfusion MR imaging at multiple delay times. *Radiology*. 2004;233:899–904.
80. Ances BM, McGarvey ML, Abrahams JM, Maldjian JA, Alsop DC, Zager EL, et al. Continuous arterial spin labeled perfusion magnetic resonance imaging in patients before and after carotid endarterectomy. *J Neuroimaging*. 2004;14:133–138.
81. Detre JA, Samuels OB, Alsop DC, Gonzalez-At JB, Kasner SE, Raps EC. Noninvasive magnetic resonance imaging evaluation of cerebral blood flow with acetazolamide challenge in patients with cerebrovascular stenosis. *J Magn Reson Imaging*. 1999;10:870–875.
82. Hajjar I, Zhao P, Alsop D, Novak V. Hypertension and cerebral vasoreactivity: a continuous arterial spin labeling magnetic resonance imaging study. *Hypertension*. 2010;56:859–864.
83. Fierstra J, Poublanc J, Han JS, Silver F, Tymianski M, Crawley AP, et al. Steal physiology is spatially associated with cortical thinning. *J Neurol Neurosurg Psychiatry*. 2010;81:290–293.
84. Hajjar I, Zhao P, Alsop D, Abduljalil A, Selim M, Novak P, et al. Association of blood pressure elevation and nocturnal dipping with brain atrophy, perfusion and functional measures in stroke and nonstroke individuals. *Am J Hypertens*. 2010;23:17–23.
85. Pollock JM, Deibler AR, Whitlow CT, Tan H, Kraft RA, Burdette JH, et al. Hypercapnia-induced cerebral hyperperfusion: an underrecognized clinical entity. *Am J Neuroradiol*. 2009;30:378–385.
86. Zaharchuk G, Bammer R, Straka M, Shankaranarayan A, Alsop DC, Fischbein NJ, et al. Arterial spin-label imaging in patients with normal bolus perfusion-weighted MR imaging findings: pilot identification of the borderzone sign. *Radiology*. 2009;252:797–807.
87. Wu B, Wang X, Guo J, Xie S, Wong EC, Zhang J, et al. Collateral circulation imaging: MR perfusion territory arterial spin-labeling at 3T. *Am J Neuroradiol*. 2008;29:1855–1860.
88. van Laar PJ, van der Graaf Y, Mali WP, van der Grond J, Hendrikse J. Effect of cerebrovascular risk factors on regional cerebral blood flow. *Radiology*. 2008;246:198–204.
89. Mandell DM, Han JS, Poublanc J, Crawley AP, Fierstra J, Tymianski M, et al. Quantitative measurement of cerebrovascular reactivity by blood oxygen level-dependent MR imaging in patients with intracranial stenosis: preoperative cerebrovascular reactivity predicts the effect of extracranial-intracranial bypass surgery. *Am J Neuroradiol*. 2011;32: 721–727.
90. Zaharchuk G, Do HM, Marks MP, Rosenberg J, Moseley ME, Steinberg GK. Arterial spin-labeling MRI can identify the presence and intensity of collateral perfusion in patients with Moyamoya disease. *Stroke.* 2011 [Epub ahead of print].
91. Heyn C, Poublanc J, Crawley A, Mandell D, Han JS, Tymianski M, et al. Quantification of cerebrovascular reactivity by blood oxygen level-dependent MR imaging and correlation with conventional angiography in patients with Moyamoya disease. *Am J Neuroradiol*. 2010;31: 862–867.
92. O'Gorman RL, Siddiqui A, Alsop DC, Jarosz JM. Perfusion MRI demonstrates crossed-cerebellar diaschisis in sickle cell disease. *Pediatr Neurol*. 2010;42:437–440.
93. Helton KJ, Paydar A, Glass J, Weirich EM, Hankins J, Li CS, et al. Arterial spin-labeled perfusion combined with segmentation techniques to evaluate cerebral blood flow in white and gray matter of children with sickle cell anemia. *Pediatr Blood Cancer*. 2009;52: 85–91.
94. van den Tweel XW, Nederveen AJ, Majoie CB, van der Lee JH, Wagener-Schimmel L, van Walderveen MA, et al. Cerebral blood flow measurement in children with sickle cell disease using continuous arterial spin labeling at 3.0-Tesla MRI. *Stroke*. 2009;40:795–800.
95. Oguz KK, Golay X, Pizzini FB, Freer CA, Winrow N, Ichord R, et al. Sickle cell disease: continuous arterial spin-labeling perfusion MR imaging in children. *Radiology*. 2003;227:567–574.
96. Villringer A, Rosen BR, Belliveau JW, Ackerman JL, Lauffer RB, Buxton RB, et al. Dynamic imaging with lanthanide chelates in normal brain: contrast due to magnetic susceptibility effects. *Magn Reson Med*. 1988;6:164–174.
97. Powers WJ, Raichle ME. Positron emission tomography and its application to the study of cerebrovascular disease in man. *Stroke*. 1985;16: 361–376.
98. Steiger HJ, Aaslid R, Stooss R. Dynamic computed tomographic imaging of regional cerebral blood flow and blood volume: a clinical pilot study. *Stroke*. 1993;24:591–597.
99. Sakai F, Nakazawa K, Tazaki Y, Ishii K, Hino H, Igarashi H, et al. Regional cerebral blood volume and hematocrit measured in normal human volunteers by single-photon emission computed tomography. *J Cereb Blood Flow Metab*. 1985;5:207–213.
100. Petersen ET, Lim T, Golay X. Model-free arterial spin labeling quantification approach for perfusion MRI. *Magn Reson Med*. 2006;55: 219–232.
101. Kim T, Kim SG. Quantification of cerebral arterial blood volume and cerebral blood flow using MRI with modulation of tissue and vessel (MOTIVE) signals. *Magn Reson Med*. 2005;54:333–342.
102. Lu H, Golay X, Pekar JJ, Van Zijl PC. Functional magnetic resonance imaging based on changes in vascular space occupancy. *Magn Reson Med*. 2003;50:263–274.
103. Gu H, Lu H, Ye FQ, Stein EA, Yang Y. Noninvasive quantification of cerebral blood volume in humans during functional activation. *Neuroimage*. 2006;30:377–387.
104. Scouten A, Constable RT. Vaso-based calculations of CBV change: accounting for the dynamic CSF volume. *Magn Reson Med*. 2008;59: 308–315.
105. Donahue MJ, Lu H, Jones CK, Edden RA, Pekar JJ, van Zijl PC. Theoretical and experimental investigation of the VASO contrast mechanism. *Magn Reson Med*. 2006;56:1261–1273.
106. Jin T, Kim SG. Spatial dependence of CBV-FMRI: a comparison between VASO and contrast agent based methods. *Conf Proc IEEE Eng Med Biol Soc*. 2006;1:25–28.
107. Donahue MJ, Hua J, Pekar JJ, van Zijl PC. Effect of inflow of fresh blood on vascular-space-occupancy (VASO) contrast. *Magn Reson Med*. 2009;61:473–480.
108. Donahue MJ, Stevens RD, de Boorder M, Pekar JJ, Hendrikse J, van Zijl PC. Hemodynamic changes after visual stimulation and breath holding provide evidence for an uncoupling of cerebral blood flow and volume from oxygen metabolism. *J Cereb Blood Flow Metab*. 2009;29: 176–185.
109. Wu CW, Liu HL, Chen JH, Yang Y. Effects of CBV, CBF, and blood-brain barrier permeability on accuracy of PASL and VASO measurement. *Magn Reson Med*. 2010;63:601–608.
110. Poser BA, Norris DG. Measurement of activation-related changes in cerebral blood volume: VASO with single-shot haste acquisition. *Magma*. 2007;20:63–67.
111. Hua J, Donahue MJ, Zhao JM, Grgac K, Huang AJ, Zhou J, et al. Magnetization transfer enhanced vascular-space-occupancy (MT-VASO) functional MRI. *Magn Reson Med*. 2009;61:944–951.
112. Poser BA, Norris DG. Application of whole-brain CBV-weighted fMRI to a cognitive stimulation paradigm: robust activation detection in a Stroop task experiment using 3D Grase VASO. *Hum Brain Mapp*. 2011;32:974–981.
113. Uh J, Lewis-Amezcua K, Martin-Cook K, Cheng Y, Weiner M, Diaz-Arrastia R, et al. Cerebral blood volume in Alzheimer's disease and correlation with tissue structural integrity. *Neurobiol Aging*. 2010;31: 2038–2046.
114. Donahue MJ, Blakeley JO, Zhou J, Pomper MG, Laterra J, van Zijl PC. Evaluation of human brain tumor heterogeneity using multiple

T1-based MRI signal weighting approaches. *Magn Reson Med*. 2008; 59:336–344.
115. Lu H, Pollack E, Young R, Babb JS, Johnson G, Zagzag D, et al. Predicting grade of cerebral glioma using vascular-space occupancy MR imaging. *Am J Neuroradiol*. 2008;29:373–378.
116. Hua J, Qin Q, Donahue MJ, Zhou J, Pekar JJ, van Zijl PC. Inflow-based vascular-space-occupancy (IVASO) MRI. *Magn Reson Med*. 2011;66: 40–56.
117. Leenders KL, Perani D, Lammertsma AA, Heather JD, Buckingham P, Healy MJ, et al. Cerebral blood flow, blood volume and oxygen utilization: normal values and effect of age. *Brain*. 1990;113:27–47.
118. van Zijl PC, Eleff SM, Ulatowski JA, Oja JM, Ulug AM, Traystman RJ, et al. Quantitative assessment of blood flow, blood volume and blood oxygenation effects in functional magnetic resonance imaging. *Nat Med*. 1998;4:159–167.
119. Stefanovic B, Pike GB. Venous refocusing for volume estimation: Verve functional magnetic resonance imaging. *Magn Reson Med*. 2005;53: 339–347.
120. Ogawa S, Lee TM, Kay AR, Tank DW. Brain magnetic resonance imaging with contrast dependent on blood oxygenation. *Proc Natl Acad Sci U S A*. 1990;87:9868–9872.
121. An H, Lin W. Quantitative measurements of cerebral blood oxygen saturation using magnetic resonance imaging. *J Cereb Blood Flow Metab*. 2000;20:1225–1236.
122. He X, Yablonskiy DA. Quantitative BOLD: mapping of human cerebral deoxygenated blood volume and oxygen extraction fraction: default state. *Magn Reson Med*. 2007;57:115–126.
123. Lee JM, Vo KD, An H, Celik A, Lee Y, Hsu CY, et al. Magnetic resonance cerebral metabolic rate of oxygen utilization in hyperacute stroke patients. *Ann Neurol*. 2003;53:227–232.
124. Lu H, Ge Y. Quantitative evaluation of oxygenation in venous vessels using T2-relaxation-under-spin-tagging MRI. *Magn Reson Med*. 2008; 60:357–363.
125. Lu H, Zhao C, Ge Y, Lewis-Amezcua K. Baseline blood oxygenation modulates response amplitude: physiologic basis for intersubject variations in functional MRI signals. *Magn Reson Med*. 2008;60: 364–372.
126. Bolar DS, Rosen BR, Sorensen AG, Adalsteinsson E. Quantitative imaging of extraction of oxygen and tissue consumption (quixotic) using venular-targeted velocity-selective spin labeling. *Magn Reson Med*. 2011 [E-pub ahead of print].

SUPPLEMENTARY MATERIAL

Human baseline and cerebrovascular reactivity cerebrovascular disease studies.

Citation	First Author	Year	MRI Technique (Parameter)	Disease	N	Clinical Significance
Stroke						
[1]	Hendrikse	2009	ASL (CBF)	Ischemia	159	159 patients with first-time symptoms consistent with cerebral ischemia were enrolled and VS-ASL was applied in conjunction with DWI. 136 patients had infarcts from DWI. RPI changed the classification of lesions in 11% of cortical or border zone infarcts, yet not for infarcts located in lacunar, periventricular, cerebellar or brainstem regions. *This work demonstrated that perfusion territory imaging with ASL can help better classify infarctions, especially in cortical and border zone regions.*
[2]	Zhao	2009	ASL (CBF)	Chronic middle cerebral artery (MCA) stroke	87	39 patients with chronic MCA territory infarcts and 48 controls were scanned using CASL to assess the extent to which vasoreactivity (in response to a CO_2 challenge) is affected by existing infarcts. It was found that patients showed a lower augmentation of CBF at increased CO_2 yet larger reduction of CBF with decreased CO_2 relative to controls. *These findings suggest that following ischemic stroke, CBF augmentation is inadequate in multiple vascular territories, yet vasocontriction is largely preserved.*
ICA disease						
[3]	Bokkers	2011	ASL (CBF)	ICA occlusion	32	CBF reactivity was investigated in patients with ICA occlusion by combining ASL-MRI with an acetazolamide vascular challenge. 16 patients with a symptomatic ICA occlusion and 16 controls underwent ASL and regional perfusion imaging before and after acetazolamide administration. Reactivity was assessed in the grey matter supplied by the unaffected asymptomatic ICA and the basilar artery. In the tissue supplied by the unaffected contralateral ICA, CVR was lower in patients when compared with the controls. *This work demonstrates that CBF reactivity can be asssessed using acetazolamide challenge, and provides regional differences in reactivity measurements between ICA occlusion patients and controls.*
[4]	Donahue	2010	iVASO (aCBV)	ICA stenosis or occlusion	25	17 patients with varying degrees of steno-occlusive disease were scanned using the aCBV-weighted iVASO approach. Elevated aCBV in the brain hemisphere from which symptoms were derived was found in 41% of patients, whereas no asymmetry was found in controls. aCBV data were also compared with Gd-DSC CBV measures, and a significant correlation was found. *This work represents the first clinical application of iVASO for assessing absolute CBV in patients with cerebrovascular disease.*

[5]	Van Laar	2008	ASL (CBF)	ICA stenosis or occlusion	130	130 patients with symptomatic atherosclerotic disease were studied to understand how cerebrovascular risk factors (body mass index, carotid artery stenosis, diabetes mellitus, hyperhomocysteinemia, hyperlipidemia, hypertension, and smoking) manifested in CBF measurements obtained using ASL. *The investigation found that in patients with symptomatic atherosclerotic disease, hypertension is directly correlated with increased CBF whereas and hyperhomocysteinemia is inversely correlated with CBF.*
[6]	Haller	2008	BOLD (CBF, CBV, CMRO2)	ICA stenosis	24	24 patients with symptomatic and high-grade ICA stenosis were recruited and scanned using BOLD in conjunction with a CO_2-challenge to understand how BOLD reactivity changed before and after CAS (n=13) or CAE (n=11). This study identified reduced BOLD reactivity in the ipsilateral MCA territory prior to treatment which normalized after treatment. Patients which developed new periinterventional infarcts exhibited the largest reduction in reactivity in the ipsilateral MCA territory prior to treatment. *This study demonstrates the potential of BOLD reactivity measurements to monitor patient responses to revascularization procedures.*
[7]	Van Laar	2007	ASL (CBF)	ICA stenosis	24	Regional perfusion imaging using ASL was performed in 24 patients with symptomatic ICA stenosis. All patients had revascularization procedures, consisting of either CAS (n=12) or CAE (n=12). It was found that the flow territory of the ipsilateral ICA in patients was smaller, and the territories of the contralateral ICA and vertebrobasilar arteries were larger compared with controls. After revascularization, differences in flow territories and CBF between patients and controls was not significant. This work demonstrates that improvements in CBF following revascularization procedures are similar for CAS and CAE.
[8]	Ziyeh	2005	BOLD (CBF, CBV, CMRO2)	ICA stenosis or occlusion	27	BOLD and transcranial Doppler measurements were made in patients with ICA stenosis, both in response to a 7% CO_2 challenge. The BOLD and Doppler reactivity were highly correlated in affected territories. *This study showed feasibility of performing BOLD reactivity measurements (here, with very high levels of administered CO_2) clinically and good correspondence with the more established transcranial Doppler technique was shown.*
[9]	Hendrikse	2004	ASL (CBF)	ICA occlusion	11	One of the shortfalls of ASL imaging in patients with steno-occlusive disease and delayed arrival times is the requirement to image late enough after the blood water labeling such that the label has had sufficient time to exchange with tissue water. *Here, ASL experiments were performed in ICA stenosis patients at multiple inversion times, demonstrating that CBF was reduced in flow territories ipsilateral to the stenosis, and more importantly, that multi-delay pulsed ASL approaches could be successfully applied clinically in patients with reduced arterial arrival times.*
Cerebrovascular risk factors						

[10]	Hajjar	2010	ASL (CBF)	Hypertension	62	The relationship between hypertensive CBF reactivity in response to a 5% CO_2 challenge was investigated using CASL in 62 volunteers. Hypertensive volunteers demonstrated reduced global reactivity, which was most significant in frontal, temporal, and parietal lobes and higher mean systolic blood pressure was associated with lower reactivity. The decrease in reactivity in patients with hypertension but no stroke was comparable to the decrease in reactivity in patients with stroke but without hypertension. *This work demonstrates that hypertension has a negative effect on cerebrovascular circulation and that this is comparable to that seen with stroke, motivating the need for studies that assess the impact of antihypertensive therapies, vasoreactivity and outcomes.*
[11]	Hajjar	2010	ASL (CBF)	Acute stroke	80	The relationship between elevated blood pressure, nocturnal dipping, brain atrophy, CBF (CASL approach) and functional status was investigated in 80 adults with and without stroke. Nocturnal dipping in systolic and pulse pressure was associated with greater brain atrophy, especially in fronto-parietal regions. Dipping in systolic blood pressure and brain atrophy were also associated with reduced gait speed and poorer recovery following stroke. Higher mean blood pressure was associated with lower CBF but not atrophy, regardless of prior history of stroke. *This study demonstrates that nocturnal dipping should be considered as an important parameter in evaluating and understanding stroke risk.*
[12]	Pollock	2009	ASL (CBF)	Hospitalized patients with hypercapnic cerebral hyperperfusion or hypocapnic hypoperfusion	45	The purpose of this study was to present clinical and CBF imaging (ASL) findings in 45 patients with hypercapnic cerebral hyperperfusion and hypocapnic hypoperfusion. Patients with hypercapnia showed global hyperperfusion on ASL and diffuse air-space abnormalities on chest radiographs. A positive linear relationship between CBF and the partial pressure of CO_2 was found. *This study suggests that owing to the noninvasive and increasingly routine implementation of ASL, hypercapnic-associated cerebral hyperperfusion will be identified more frequently and may provide diagnostic information for certain neuropsychiatric symptoms.*
[13]	Zaharchuk	2009	ASL (CBF)	Cerebrovascular disease	139	The goal of this study was to understand whether CBF (pCASL) abnormalities are depicted on ASL images obtained in patients with Gd-DSC MRI. 41 patients had normal Gd-DSC findings, with 56% of these patients having normal ASL findings. The remaining 44% patients had the ASL borderzone sign and had lower mean CBF compared with the patients who had normal ASL imaging findings. Approximately half of the patients with normal Gd-DSC findings had abnormal ASL findings-most commonly the borderzone sign. *Results of this study suggest that ASL yields additional information to Gd-DSC.*
[14]	Wu	2008	Vessel-encoded	ICA and/or MCA	56	The aim of this study was to investigate distal flow of collaterals using VS-ASL) in

			ASL (CBF)	stenosis		56 patients with either ICA or MCA stenosis. *In this patient population, VS-ASL could identify the presence and origin of collateral flow, thereby demonstrating feasibility of VS-ASL for understanding collateralization in patients with large-vessel steno-occlusive disease.*
[15]	Van Laar	2008	ASL (CBF)	Vascular risk factors	121	The study evaluated the effect of growth factors on CBF in humans using ASL. Circulating levels of vascular endothelial growth factor (VEGF), granulocyte-macrophage colony-stimulating growth factor (GM-CSF), tumor necrosis factor alpha (TNFα) and basic fibroblast growth factor (bFGF), along with CBF measurements, were recorded in 121 patients with symptomatic atherosclerotic disease. *Increasing levels of TNFα were significantly associated with a higher CBF, independent of cerebrovascular risk factors. No correlation was found between CBF and VEGF, GM-CSF or bFGF.*
Intracranial stenosis						
[16]	Mandell	2011	BOLD (CBF, CBV, CMRO2)	Intracranial stenosis with EC/IC Bypass	25	The aim of this study was to determine whether preoperative BOLD reactivity measurements in response to CO_2 challenge could predict the hemodynamic effect of EC/IC bypass in 25 patients with intracranial steno-occlusive disease. BOLD reactivity was measured preoperatively and postoperatively. Patients with normal preoperative reactivity demonstrated no significant change in reactivity following bypass surgery, whereas patients with reduced preoperative reactivity showed improvement following surgery, and patients with paradoxical preoperative reactivity showed the largest change following surgery. *This study suggests that preoperative measurement BOLD reactivity measurements predict the hemodynamic response to EC/IC bypass in patients with intracranial steno-occlusive disease.*
[17]	Zaharchuk	2011	ASL (CBF)	Moyamoya	18	The purpose of this study was to determine how ASL compared with digital subtraction angiography (DSA) and Xe CT for assessing collateral flow in 18 patients with Moyamoya disease. Agreement between ASL and DSA consensus readings was moderate to strong and sensitivity and specificity for identifying collaterals with ASL were 0.83 and 0.82; Xe CT CBF increased with increasing DSA and ASL collateral grade. *This study demonstrates that similar to DSA, ASL can predict the presence of collateral flow in patients with Moyamoya disease.*
Sickle cell disease						
[18]	Oguz	2003	ASL (CBF)	Sickle cell disease	14	One of the earlier studies using ASL in sickle cell disease. CBF was measured with CASL in 14 children with sickle cell disease. Mean CBF values were higher in patients than controls in all flow territories evaluated, however variations between patients were found. Specifically, three patients had decreased CBF in right anterior and middle cerebral artery territories, and one patient had decreased CBF in all right hemisphere territories. *This study demonstrated that ASL was feasible in sickle*

						cell disease studies, and that regional variability in CBF could provide an important measurement in understanding disease severity and progression.

References

1. Hendrikse J, Petersen ET, Cheze A, Chng SM, Venketasubramanian N, Golay X. Relation between cerebral perfusion territories and location of cerebral infarcts. *Stroke*. 2009;40:1617-1622
2. Zhao P, Alsop DC, Abduljalil A, Selim M, Lipsitz L, Novak P, et al. Vasoreactivity and peri-infarct hyperintensities in stroke. *Neurology*. 2009;72:643-649
3. Bokkers RP, Wessels FJ, van der Worp HB, Zwanenburg JJ, Mali WP, Hendrikse J. Vasodilatory capacity of the cerebral vasculature in patients with carotid artery stenosis. *AJNR Am J Neuroradiol*. 2011;32:1030-1033
4. Donahue MJ, Sideso E, MacIntosh BJ, Kennedy J, Handa A, Jezzard P. Absolute arterial cerebral blood volume quantification using inflow vascular-space-occupancy with dynamic subtraction magnetic resonance imaging. *J Cereb Blood Flow Metab*. 2010;30:1329-1342
5. van Laar PJ, van Raamt AF, van der Grond J, Mali WP, van der Graaf Y, Hendrikse J. Increasing levels of tnfalpha are associated with increased brain perfusion. *Atherosclerosis*. 2008;196:449-454
6. Haller S, Bonati LH, Rick J, Klarhofer M, Speck O, Lyrer PA, et al. Reduced cerebrovascular reserve at co2 bold mr imaging is associated with increased risk of periinterventional ischemic lesions during carotid endarterectomy or stent placement: Preliminary results. *Radiology*. 2008;249:251-258
7. Van Laar PJ, Hendrikse J, Mali WP, Moll FL, van der Worp HB, van Osch MJ, et al. Altered flow territories after carotid stenting and carotid endarterectomy. *J Vasc Surg*. 2007;45:1155-1161
8. Ziyeh S, Rick J, Reinhard M, Hetzel A, Mader I, Speck O. Blood oxygen level-dependent mri of cerebral co2 reactivity in severe carotid stenosis and occlusion. *Stroke*. 2005;36:751-756
9. Hendrikse J, van Osch MJ, Rutgers DR, Bakker CJ, Kappelle LJ, Golay X, et al. Internal carotid artery occlusion assessed at pulsed arterial spin-labeling perfusion mr imaging at multiple delay times. *Radiology*. 2004;233:899-904
10. Hajjar I, Zhao P, Alsop D, Novak V. Hypertension and cerebral vasoreactivity: A continuous arterial spin labeling magnetic resonance imaging study. *Hypertension*. 2010;56:859-864
11. Hajjar I, Zhao P, Alsop D, Abduljalil A, Selim M, Novak P, et al. Association of blood pressure elevation and nocturnal dipping with brain atrophy, perfusion and functional measures in stroke and nonstroke individuals. *Am J Hypertens*. 2010;23:17-23
12. Pollock JM, Deibler AR, Whitlow CT, Tan H, Kraft RA, Burdette JH, et al. Hypercapnia-induced cerebral hyperperfusion: An underrecognized clinical entity. *AJNR Am J Neuroradiol*. 2009;30:378-385
13. Zaharchuk G, Bammer R, Straka M, Shankaranarayan A, Alsop DC, Fischbein NJ, et al. Arterial spin-label imaging in patients with normal bolus perfusion-weighted mr imaging findings: Pilot identification of the borderzone sign. *Radiology*. 2009;252:797-807
14. Wu B, Wang X, Guo J, Xie S, Wong EC, Zhang J, et al. Collateral circulation imaging: Mr perfusion territory arterial spin-labeling at 3t. *AJNR Am J Neuroradiol*. 2008;29:1855-1860
15. van Laar PJ, van der Graaf Y, Mali WP, van der Grond J, Hendrikse J. Effect of cerebrovascular risk factors on regional cerebral blood flow. *Radiology*. 2008;246:198-204
16. Mandell DM, Han JS, Poublanc J, Crawley AP, Fierstra J, Tymianski M, et al. Quantitative measurement of cerebrovascular reactivity by blood oxygen level-dependent mr imaging in patients with intracranial stenosis: Preoperative cerebrovascular reactivity predicts the effect of extracranial-intracranial bypass surgery. *AJNR Am J Neuroradiol*. 2011;32:721-727
17. Zaharchuk G, Do HM, Marks MP, Rosenberg J, Moseley ME, Steinberg GK. Arterial spin-labeling mri can identify the presence and intensity of collateral perfusion in patients with moyamoya disease. *Stroke*. 2011. [E-pub ahead of print].
18. Oguz KK, Golay X, Pizzini FB, Freer CA, Winrow N, Ichord R, et al. Sickle cell disease: Continuous arterial spin-labeling perfusion mr imaging in children. *Radiology*. 2003;227:567-574

Full Article

허혈 뇌혈관질환에 있어 뇌혈류역학의 평가에 대한 참신한 MRI적 접근

Novel MRI Approaches for Assessing Cerebral Hemodynamics in Ischemic Cerebrovascular Disease

Manus J. Donahue, PhD; Megan K. Strother, MD; Jeroen Hendrikse, MD, PhD

(*Stroke*. 2012;43:903-915.)

Key Words: cerebral blood flow ■ cerebral blood volume ■ cerebral hemodynamics ■ stroke ■ stenosis ■ cerebrovascular disease ■ MRI

뇌혈류역학의 변화는 다양한 허혈 뇌혈관질환의 기초가 된다. 혈류역학적(뇌혈류 및 뇌혈액량) 및 대사성(뇌산소대사율) 지표를 정확하고 정량적으로 측정할 수 있는 능력은 건강한 뇌의 기능 및 허혈에서의 상대적인 기능 이상을 이해하는 데 있어 중요하다. PET, SPECT 및 조영증강 MRI를 통한 접근이 일반적이기는 하나, 외인성 조영제를 필요로 하지 않는 보다 최근의 MRI적 접근이 혈류역학적 지표에 대해 다양한 민감성을 가지고 소개되고 있다. 이러한 최신의 접근법을 가지고 혈류역학적 측정을 얻을 수 있는 능력은 추적 혹은 종적 연구가 필요한 임상적 혹은 실험적 연구에 있어 더욱 호소력이 있다. 이 리뷰의 목적은 뇌혈류(CBF), 뇌혈액량(CBV) 및 뇌산소대사율($CMRO_2$) 측정에 대한 최첨단 MRI 방법에 대해 개요를 서술하고 영상학적 함정을 피하기 위한 실제적 조언을 제공하는 데 있다. 외인성 조영제 없이 시행된 뇌혈관질환에 대한 MRI 연구들이 임상적 합당성 및 방법론적 장단점의 측면에서 요약되어 있다.

이 리뷰의 목적은 뇌혈관질환에서의 CBF, CBV, $CMRO_2$ 및 산소추출률(oxygen extraction fraction, OEF)을 평가하는 데 이용될 수 있는 비침습적(조영제 주입 없는) MRI 방법에 대한 논의를 하는 데 있다. 이러한 다양한 방법들은 이전에 확립된 침습적 방법에 비교할 만한 대비를 보여주고 있으며, 급성 혹은 만성 허혈 환자에서 조직 수준에서의 혈류역학을 규정하는 데 적합한 방법으로 사용되고 있다.

생리적으로 뇌관류압(cerebral perfusion pressure, CPP)이 감소하면서 조직 수준에서의 혈류역학적 악화의 정도는 CBV를 증가시키고 CBF를 보충하기 위한 측부순환의 발달을 위한 혈관의 자동조절 능력을 반영하게 된다. CBV와 OEF에서의 국소변이와 함께 CBF 곁순환화(collateralization)는 특별히 뇌졸중의 위험도와 연관된다는 가설이 제시되고 있는데, 이를 뒷받침하는 것으로는 이러한 위험도가 증가된 CBV와 OEF가 양의 상관관계가 있다라는 증거가 제시되었다.[1] CBF, CBV, OEF 및 $CMRO_2$의 정밀한 측정은 뇌혈관질환의 진행과 관련한 중요한 단서를 제공하고 있으며,[2,3] 혈류역학적 악화에 대한 정확한 측정은 진단 및 위험도의 계층화를 향상시킬 수 있는 가능성을 가지고 있다.[1] 그러나 혈류역학적 측정법은 뇌혈관질환의 급성 혹은 장기적 평가에 대해 표준화되어 있지 않다. 이것을 이루기 위해서 극복해야 할 중요한 장벽으로는 (1) 고도의 특이도 및 유용성을 가진 조직 혈류역학에 대한 방법론의 부재 및 (2) 손상의 장기적인 진행을 추적할 수 있는 비침습적 방법의 부재를 들 수 있다.

최근 뇌혈류역학상태에 대한 정량적 정보를 제공을 표방한 새로운 MRI 방법들이 개발되고 있으나 실제로는 아직까지 재

From the Department of Radiology (M.J.D., M.K.S.), the Department of Psychiatry (M.J.D.), and the Department of Physics (M.J.D.), Vanderbilt University, Nashville, TN; and the Department of Radiology, University Medical Center Utrecht, The Netherlands (J.H.).

The online-only Data Supplement is available with this article at http://stroke.ahajournals.org/lookup/suppl/doi:10.1161/STROKEAHA.111.635995/-/DC1.

Correspondence to Manus J. Donahue, PhD, Psychiatry, Physics, Radiology and Radiological Sciences, 1161 21st Ave S, MCN, AAA-3115, Nashville, TN 37232–2310. E-mail mj.donahue@vanderbilt.edu

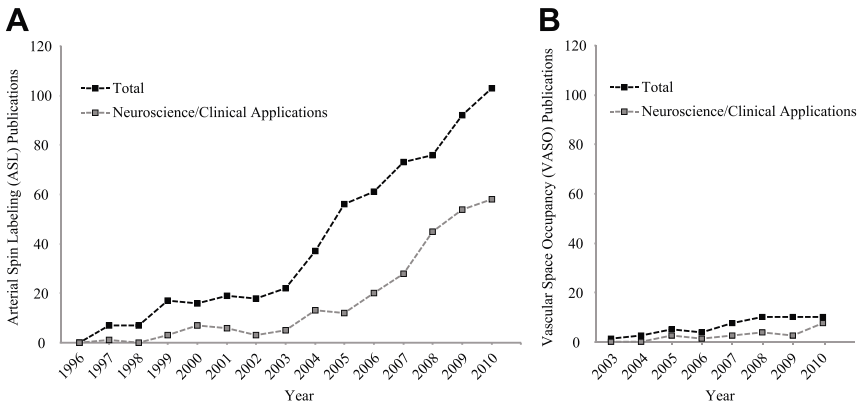

Figure 1. The growing popularity of non-invasive hemodynamic MRI. **A**, Yearly total number of arterial spin labeling (ASL), and **B**, vascular-space-occupancy (VASO) publications since 1996 (ASL) and 2003 (VASO) and corresponding total number of non-methodological studies of these techniques where the focus was specifically to use the method for addressing a neurophysiological question.

현성 및 적용의 편의성은 가변적이다. 이러한 기법과 기존의 구조적 스캔의 결합을 통한 최신의 MRI 프로토콜은 이론적으로 조직 수준 질환의 단계 및 뇌경색의 분포 및 크기에 대한 정보를 모두 제공할 수 있다. 최근의 MRI 방법에 대한 개요가 정상인 혹은 일부 환자들에게 시행된 PET과 SPECT과의 비교를 통해 제시되어 있다. 이러한 MRI 접근법에 대한 정확성, 효용성, 전문지식 및 임상적 타당성이 뇌혈관질환의 맥락에서 요약되어 있다.

혈류역학 MRI: State of the Field

혈류역학적 손상을 평가하기 위한 표준 검사는 CBF, CBV, OEF 등이 있으며, $CMRO_2$에 대해서는 PET 검사, 추가적인 CBF나 CBV에 대한 측정으로는 SPECT를 이용할 수 있다. 그러나 PET와 SPECT를 통한 측정은 환자에 대한 진단적 방법으로 자주 수행되지는 않는데, 그 이유로 일상적 적용에 있어 어려움이 있고 일부 비특성화 센터에서는 사용이 불가능한 외인적 추적자가 필요함 등을 들 수 있다. MRI는 PET와 SPECT에 비해 폭넓게 사용되고 촬영도 빠르다. 확산강조영상(diffusion-weighted imaging, DWI)과 액체감쇠역전회복영상(fluid attenuated inversion recovery, FLAIR)은 작거나 큰 급성, 아급성 혹은 오래 지속되는 허혈성 뇌경색을 확인하는 데 현재까지 가장 민감도가 높은 검사이다. 급성기 뇌졸중의 표준 검사이며 높은 진단적 정확도를 가지고 있는 DWI는 2분 미만의 스캔 시간이 필요하다.[4]

관류 MRI는 혈류역학적 이상에 대한 추가적인 정보를 전달한다. 대부분의 MRI 관류검사는 gadolinium (Gd)-역동적 감수성 대비(dynamic susceptibility contrast, DSC)를 이용하는데 Gd 킬레이트는 4-6 mL/s의 속도로 정맥으로 주입되며 90~120초 동안 단일 기울기에코 영상(TR/TE1.5/0.03초)을 추적하여 얻게 된다. 신호의 일시적 변화를 추적자동태모형에 적용하여 mean transit-time (MTT), time-to-peak (TTP), CBV 그리고 보다 적게는 CBF 정량화를 가능하게 한다. Gd-DSC는 만성 혹은 허혈성 뇌혈관질환에서 대규모로 사용되고 있는데 많은 리뷰가 이용 가능하다.[5,6] 관류/확산 부정합과 뇌경색 위험도에 따라 환자들을 구분하는 데 있어 Gd-DSC를 이용한 최근의 급성 뇌졸중 임상시험으로는 Desmoteplase in Acute Ischemic Stroke (DIAS) 연구,[7] DIAS-2 연구,[8] Dose Escalation of Desmoteplase for Acute Ischemic Stroke (DEDAS) 연구[9] 및 Diffusion and Perfusion Imaging Evaluation for Understanding Stroke Evolution (DEFUSE) 연구 등이 있다.[10]

Gd-DSC 영역에서 계속 진행되고 있는 개발들은 자동화된 후처리프로그램 및 허혈 전후의 조직의 운명을 예측할 수 있는 알고리즘의 관련 평가에 집중하고 있다. 어떠한 소프트웨어 조합도 모든 상황에서 조직의 운명을 확실히 예측하는 것은 불가능하나 새로운 CBF 역치화 접근 및 자동화 분석 소프트웨어는 재관류[11]에 대한 차별적 반응을 예측하고 경색으로 진행하는 뇌조직의 낮은 경계를 예측하는 것에 대한 장래성을 보여주고 있다.[12]

그러나 Gd-DSC는 조영제의 주입을 필요로 하는데 이는 신성 전신성 섬유화(nephrogenic systemic fibrosis)와의 연관성으로 인하여 과거 10년 동안 사용에 제한적일 수 밖에 없었다.[13] 신부전 환자와 같이 Gd 기반 조영제의 사용이 금기된 환자들의 임상 연구에서는 Gd-DSC는 일반적으로 연구 목적으로 허용되지 않는다. 또한 용량한계로 인하여 다수의 반복적인 검사가 요구되는 종적 연구에서 Gd-DSC의 사용은 제한적이다. 그러므로 Gd 기반 조영제를 필요로 하지 않는 새로운 접근을 사용하는 리서치 연구들이 점차 증가하고 있다.

CBF 평가에 대한 새로운 MRI 접근

동맥스핀라벨(arterial spin labeling, ASL) MRI[14]는 CBF를 측정하는 데 있어 외인성 조영제를 필요로 하지 않는 가장 잘 알려진 MRI 기법으로 최근 많은 수의 방법론과 이를 이용한 임상연구가 시행되고 있다(Figure 1). ASL에서는 조직 근위부의 혈액내 물에 고주파 펄스(radiofrequency pulse)를 사용하게 된다. 고주파가 표지된 혈액 물 내의 양성자는 뇌 조

Table 1. Hemodynamic Methods Comparison

Citation	First Author	Year	MRI Technique (Parameter)	Reference Technique (Parameter)	Population	n	Findings
19	Noguchi	2011	ASL (CBF)	SPECT (CBF)	Moyamoya	12	Hemispherical CBF correlated between ASL and SPECT
20	Liu	2011	ASL (CBF)	SPECT (CBF)	Gulf war illness	47	CBF trends similar between ASL and SPECT (SPECT data from separate study)
21	Uh	2011	VASO (CBV)	PET (CBV)	Controls	8	CBV similarity between VASO and PET
22	Donahue	2010	iVASO (CBV)	Gd-DSC	ICA steno-occlusion	17	CBV correlation between iVASO and Gd-DSC
23	Wissmeyer	2010	ASL (CBF)	PET (CBF)	Epilepsy	3	CBF correlation between ASL and PET
24	Xu	2010	ASL (CBF)	PET (CBF)	Elderly controls	9	Global and regional CBF agreement between ASL and PET
25	Qiu	2010	ASL (CBF)	PET (CBF)	Controls	14	Variations in AAT influence regional ASL CBF quantification
26	Bokkers	2010	ASL (CBF)	PET (CBF)	ICA occlusion	14	CBF overestimation in ASL relative to PET
27	Knutsson	2010	ASL (CBF)	Gd-DSC	Brain tumor	15	Linear correspondence between ASL and Gd-DSC
28	Lüdemann	2009	ASL (CBF)	PET (CBF)	Glioma	12	CBF measured most reliably with ASL compared to other methods
29	Chen	2008	ASL (CBF)	PET (CBF)	Controls	10	CBF correlation between ASL and PET; ASL yielded slightly lower CBF
30	Newberg	2005	ASL (CBF)	PET (CMR_{Glc})	Controls	5	Concordance between ASL CBF and PET-measured cerebral metabolic rate of glucose
31	Kimura	2005	ASL (CBF)	PET (CBF)	ICA occlusion	11	ASL and PET correlation; ASL CBF underestimation ipsilateral to the carotid occlusion
32	Wintermark	2005	ASL (CBF)	PET, SPECT, Gd-DSC	Multiple	. . .	Review of perfusion imaging techniques
33	Weber	2003	ASL (CBF)	Gd-DSC	Brain metastases	62	Comparable CBF contrast in healthy tissue found using ASL and Gd-DSC
34	Liu	2001	ASL (CBF)	PET (CBF)	Epilepsy	8	Correlation between ASL and PET hypoperfusion
35	Ye	2000	ASL (CBF)	PET (CBF)	Control subjects	12	Gray matter CBF similar between ASL and PET; white matter CBF underestimated with ASL

ASL indicates arterial spin labeling; CBF, cerebral blood flow; SPECT, single-photon computed tomography; VASO, vascular-space-occupancy; PET, positron emission tomography; CBV, cerebral blood volume; ICA, internal carotid artery; Gd-DSC, gadolinium–dynamic susceptibility contrast.

직을 돌아다니면서 조직내 물과 교환하게 된다. 결과적으로 조직내 물의 자화에 작은 감쇄가 일어나게 되고 이는 교환이 일어난 정도인 CBF에 비례하게 된다. 그러나 표지펄스가 가해질 때의 자화의 변화는 상대적으로 전체 총 신호량에 비해 상당히 작다. 따라서 표지 동안 얻어진 영상은 대조(비표지) 영상으로부터 감산처리가 이루어진다. 이후 추적자 동역학 모델[15]이 ASL 신호 차이에 적용되어 분당 100 g의 조직 내에 혈액이 얼마나 들어왔는지(absolute units of mL blood/100 g tissue per minute) CBF를 정량화한다.

ASL의 원리는 $H_2{}^{15}O$ PET CBF의 측정과 유사한 방법으로[16]

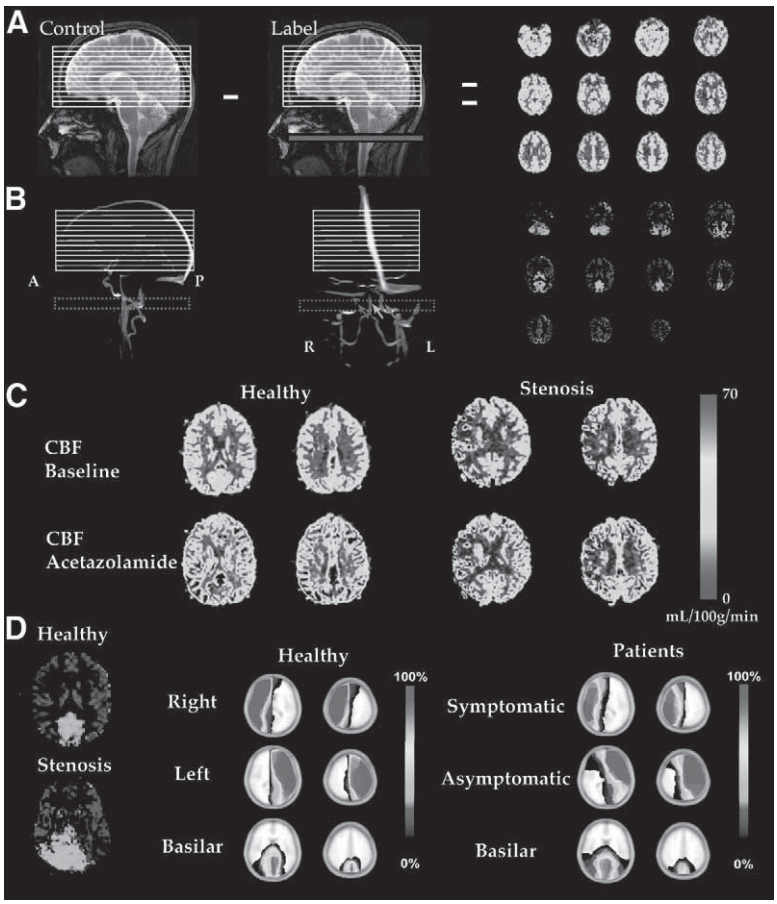

Figure 2. Cerebral blood flow (CBF) imaging using arterial spin labeling (ASL) MRI. **A**, Pseudocontinuous ASL (pCASL) approach in which CBF-weighted maps are obtained from subtraction of a labeled (red) blood water acquisition from an unlabeled control acquisition. **B**, Vessel-selective ASL in which blood water is separately labeled in right internal carotid artery (ICA) (red), left ICA (blue), and basilar (green) arteries; **right**, corresponding CBF maps are generated. **C**, Example baseline and acetazolamide pCASL-CBF maps for a healthy volunteer and a patient with symptomatic right ICA stenosis. **D**, Vessel-selective pCASL shows altered posterior and right flow territories in a patient with right ICA stenosis. **Right**, Axial flow-territory maps projected on a standardized atlas for healthy control participants (n=20) and patients with symptomatic ICA stenosis (n=23). Scale indicates percentage of individuals in the denoted group with measured perfusion.

두 방법 모두 자유확산 추적자 기반 방법(freely diffusible tracer-based approach)을 이용한다. 그러나 PET에서의 추적자는 주입된 H_2인 반면 ASL에서의 추적자는 내인적인 혈액내 물이다. PET에서의 ^{15}O의 반감기는 약 2분인 반면 ASL에서의 혈액물추적자는 혈액물의 세로완화시간(T_1)이 짧아 빨리 감쇄가 일어난다. 1.5 T에서는 1.2초로 짧은 반면 3.0 T와 7.0 T에서는 각각 1.7초와 2.5초로 늘어나게 된다.[17] ASL에서는 내인적 추적자의 상대적으로 빠른 감쇄로 인하여 짧은 기간(4~8초)내에 반복적 측정을 할 수 있으며 신경 혹은 혈관에 의한 CBF의 변화도 측정할 수 있다.[18] Table 1에 각각의 방법에 대한 비교가 나와있는데 이 중 ASL, PET, SPECT 및 DSC 사이의 CBF는 비슷한 것으로 보고하고 있다.

ASL 접근방법은 어떻게 표지를 하는지에 따라 펄스 ASL (PASL)와 연속 ASL (CASL) 두 가지로 구분할 수 있다.[36] PASL과 CASL의 차이점은 표지하는 방식의 차이인데 PASL은 3~15 ms 동안 한 번[37] 혹은 두 번[38]의 고주파펄스가 경부에서 큰 용적(80~120 mm)의 혈액에 표지가 이루어지나 CASL은 1.5~2초 동안의 긴 표지 펄스가 목의 한 부위에서 일어나게 된다는 차이점이 있다.[39,40] CASL의 신호대잡음비는 PASL 방법에 비해 30~50% 높기 때문에[41] 원칙적으로는 CASL이 더욱 바람직하다. 그러나 PASL 방법은 짧은 펄스가 표준 MRI 몸통코일로 발생 가능하며, 반면 CASL의 긴 펄스는 새로운 국소전송코일이 요구되므로 실제로는 PASL 방법이 더 많이 사용되고 있다.[42]

PASL MRI에서 CBF 측정은 표지지역과 관심영상지역 사이의 거리에 의존하게 되는데[43] 이는 뇌의 각 부위마다 다양하다. 예를 들어 영양동맥의 말단가지에 의해 혈액을 공급받는 경계구역 혹은 분수계지역은 혈액내 물이 표지된 지역으로부터 모세혈관교환부위로 이동하는 데 걸리는 시간, 즉 동맥도착시간(arterial arrival time, AAT)이 늘어나게 된다. AAT는 대략 500~1,100 ms 정도[44,45]로 동맥 폐색과 측부혈류를 가지고 있는 환자에게서는 증가할 수 있다.[46,47] 긴 AAT 값은 혈액내 물이 조직에 도달하지 않을 경우 CBF가 과소평가될 수 있다. 두개내 죽경화성 협착 혹은 모야모야 양상의 혈관을 가진 환자에서 ASL 방법은 늘어난 AAT에 의해 혈관내신호가 증가하게 된 혈관과 인접한 국소지역의 CBF를 과대평가할 수 있다. 이를 해결하기 위해 PASL 데이터들은 일반적으로 300~2,500 ms의 다수의 표지후지연시간(postlabeling delay times) 방법을 통하여 AAT와 CBF의 동시 정량화를 가능하게 한다. 이 접근법의 실행가능성은 협착-폐색환자에서 증명이 되었고[46,48] SPECT 검사와의 비교를 통해 입증되었다.[25,27] 그러나 다중표지지연으로 얻어지는 ASL의 경우 단일지연 접근법

에 비해 추가적인 스캔시간이 요구된다. 단일표지후지연으로 뇌전체영상을 얻는 데 2~4분이 걸리는 반면 다중지연법으로 비교할만한 영상을 얻는 데는 5~8분 정도의 시간이 요구된다. 신호의 빠른 감쇄는 ASL 추적자표지가 극복해야 하는 문제일 수 있으나 이러한 빠른 신호감쇄는 Gd-DSC, PET 혹은 SPECT로부터 얻어질 수 없는 신경 혈관 임무(task)[18]에 대한 CBF의 변화를 측정하는 데에 중요한 요소가 된다.

최근 개선된 ASL법으로 거짓연속 ASL (pCASL) 방법이 있다.[41] pCASL (Figure 2)에서는 표지가 CASL과 같이 긴 시간 동안 이루어지지만 짧은 연속된 펄스가 반복적으로 이루어지게 된다. 이러한 짧아진 펄스는 기존의 몸통코일에 적용할 수 있고 CASL에 비교할 만한 신호대잡음비를 제공할 수 있다.[41] pCASL 방법은 최근에 사용이 많아지고 있으며 병원 MRI를 이용한 ASL 방법 중에 있어서 가장 널리 쓰이는 방법이 될 것이다. pCASL은 높은 신호대강도비를 유지하고 있으며 PASL에 비해 AAT에 덜 민감하다.

ASL법은 정상 CBF의 주변지역과 확실히 구분되는 대뇌피질과 같은 곳의 CBF의 감소를 측정하는 데에 더욱 유용할 것이다. 반대로 백색질의 CBF는 회색질의 CBF에 비해 2~3배 적고 AAT는 1.5~2.5초로 길다. 따라서 백색질의 신호는 주변 잡음 수준보다 바로 위 정도의 신호강도를 가지게 되므로[49] 저관류된 백색질을 찾는 것은 어렵다. AAT 지연으로 인한 단점이 최근 개발된 속도 선택적 ASL (velocity-selective ASL) 방법으로 극복될 수 있다. 이 방법으로 감쇄된 동맥내 혈액이 뇌조직에 가까운 부위에서 표지하여 AAT 지연으로 인한 신호손실을 줄일 수 있는 장점이 있다.[50]

또한 최근 개발되고 있는 방법으로 혈관 선택적 ASL (vessel-selective ASL, VS-ASL)이 있다. 이 방법에서는 다양한 영양혈관(일반적으로 좌/우 속목동맥 혹은 뇌바닥동맥)을 각각 분리하여 표지시켜 관류된 지역 및 측부순환을 측정할 수 있다.[51,52] 이러한 접근법(Figure 2)이 최근 가장 개발이 집중되고 있는 분야이며 뇌혈관질환의 가진 환자의 보상적 혈류패턴을 분석하기 위해 성공적으로 적용되어오고 있다.[53]

ASL 방법의 기술적 진전으로 인해 위에서 언급된 표지전락에 대해서도 보완이 이루어지고 있다. 배경최소화(background suppression)법은 정적인 흑색질과 백색질의 신호를 감소시키는 방법으로 대부분의 ASL 방법에서의 신호대잡음비를 개선시킬 수 있다.[54,55] 또한 분쇄구배법(crusher gradient)도 ASL 영상을 얻을 때 큰 혈관에서의 동맥 신호를 최소화시켜 혈관내 혈액 물로부터의 오염 없이 CBF의 대비를 향상시킬 수 있다. 다양한 영상 정보읽기방법도 역시 이용 가능하다. 가장 일반적인 방법으로는 단사(2D) 에코평면영상(echo planar imaging, EPI)을 들 수 있다. 그러나 2D 영상정보읽기를 통해 뇌전체 영상을 얻는 데에는 어려움이 많다. 즉 요구되는 다수의 활성펄스가 절편에 의존적인 표지지연을 가져와 CBF 정량화를 어렵게 만드는 단점이 있다. 3차 GRadient and Spin Echo (GRASE) 영상정보처리가 이러한 절편-시점 불일치를 제거하기 위해 적용되고 있다.[56] 2D EPI에 비교하여 3D GRASE 영상처리는 신호대잡음비를 200~300배 증가시킨다.[56] 3D GRASE를 적용한 ASL 방법이 정상 자원자들에서 기초,[57,58] 약리학[59] 및 신경혈관 결합,[18] 또한 경동맥 협착-폐색환자들[46]의 CBF 변화를 조사하기 위해 적용되고 있다.

많은 다양한 인체대상연구에서 ASL은 뇌혈관질환에서 CBF의 변이를 평가하기 위해 사용되고 있다(Table 2). 지난 10년간의 성과에 힘입어 ASL 방법은 3.0 T의 자기장에서도 적용되어 전체 뇌의 CBF를 신뢰할 만한 수준으로 얻을 수 있게 되었다. 최근 성공적인 ASL 연구들이 1.5 T보다는 3.0 T MRI에서 많이 시행되고 있다. 이것은 3.0 T의 자기장에서 혈액내 물의 T_1이 길어지고(표지기간의 연장) 3.0 T에서의 신호대잡음비가 증가하기 때문이다.

배경최소화와 혈류분쇄구배와 함께 2D 혹은 3D 영상처리 기법들을 동원하여 pCASL을 시행한 결과 PET과 SPECT에 비교할 만한 CBF값을 얻을 수 있게 되었다. 그러나 PET 혹은 SPECT와는 달리 ASL 연구들은 3~5분만에 촬영이 가능하고 3~5 mm의 등방성 복셀크키를 가지는 높은 공간해상도에 더하여 VS-ASL에서는 피질리본과 작은 피질하 구조들에서의 부분용적효과를 최소화할 수 있으며 측부혈류의 동태에 관련된 추가적인 정보를 전해줄 수 있는 장점이 있다.

뇌혈액량(Cerebral Blood Volume)

인체의 전체 CBV 정량화는 침습적인 조영제를 사용하거나 Gd-DSC,[96] PET,[97] CT[98] 혹은 SPECT[99]를 이용하여 가능하다. 따라서 내인성 조영제를 사용하여 신경 자극에 따른 전체 및 정맥 내 CBV 반응을 측정하기 위한 MRI 접근법이 제안되었고 ASL MRI 방법이 그 추정을 위해 수정되어 적용되고 있다.[100,101] 그러한 방법들은 조영제 기반 기술의 결과와 비교하여 재현성이 높고 비교할 만한 결과들을 제공할 수 있으며 협착-폐색질환의 임상 영상에 대한 기대를 가능하게 한다.

특히 vascular-space-occupancy (VASO) MRI는 증가된 신경활성과 연관된 CBV 적응반응을 비침습적으로 측정하는 것이 가능하도록 한다.[102] VASO에서 혈액 물 신호는 영(null) 신호로 되어있어, 결과적인 영상은 원천적으로 혈관외 조직으로부터의 영상만을 포함하고 있다. 측정된 조직신호의 감소는 신경활성에 동반된 혈관분획량의 증가로 계산된다. VASO 대비 메커니즘이 연구되면서 신호변화,[103-105] 뇌척수액에 의한 오염,[104,105] 다른 CBV 가중 접근법의 일관성,[106] 혈류와 T_1변이[107] 및 임상적 실현가능성에 대한 연구들이 진행되고 있다. VASO는 ASL (2003년에 최초로 게재됨, Figure 1)에 비해 덜 대중적이나 개발 이후의 시간대에서는 ASL과 유사할 정도로 그 인기가 증가하고 있다. VASO 대비와 더욱 잘 확립되어 있는 mono-

Table 2. Human Baseline and Reactivity Cerebrovascular Disease Studies

Citation	First Author	Year	MRI Technique (Parameter)	Disease	n	Findings
Stroke						
46	MacIntosh	2010	ASL (CBF, AAT)	Acute minor stroke or TIA	30	Reduced CBF and increased AAT in patients relative to controls
60	Chen	2009	ASL (CBF)	Pediatric ischemic stroke	10	Acute and follow-up infarct volumes largest in cases with hypoperfusion
61	Hendrikse*	2009	ASL (CBF)	Ischemia	159	ASL provides diagnostic capability in 92% of patients
62	Zhao*	2009	ASL (CBF)	Chronic middle cerebral artery stroke	87	Despite preserved vasoconstriction, CBF augmentation is inadequate in many vascular territories in patients with large-artery ischemic disease
63	Pollock	2008	ASL (CBF)	Anoxic injury	16	Gray matter CBF significantly higher in anoxic injury subjects
64	Wolf	2003	ASL (CBF)	Acute and/or chronic cerebrovascular disease	10	Invasive CBF measurements correlated with ASL CBF measurements in patients who did not have major transit time delays
65	Chalela	2000	ASL (CBF)	Acute ischemic stroke	15	ASL detects perfusion/diffusion (DWI) mismatches in acute ischemic stroke patients
66	Detre	1998	ASL (CBF)	Stroke, TIA, or severe ICA stenosis	14	Good-quality CBF-weighted maps can be obtained using ASL in patients
ICA disease						
67	Bokkers*	2011	ASL (CBF)	ICA occlusion	32	ASL identified regional impaired acetazolamide-induced cerebrovascular reactivity in patients relative to control subjects
68	Hartkamp	2011	ASL (CBF)	ICA stenosis	53	Caudate nucleus is supplied with blood by the contralateral ICA more frequently in patients than control subjects
69	Bokkers	2010	ASL (CBF)	ICA stenosis	43	Vasodilatory capacity and regional variability in flow territories of major cerebral arteries can be visualized with ASL
26	Bokkers	2010	ASL (CBF)	ICA occlusion	14	ASL at multiple delay times depicts areas of reduced CBF in patients; overestimation of CBF relative to $H_2{}^{15}O$ PET was noted
22	Donahue*	2010	iVASO (arterial CBV)	ICA stenosis or occlusion	25	Arterial CBV elevated in brain hemisphere from which symptoms were derived in 41% of patients; no asymmetry found in control subjects
70	Donahue	2009	VASO (CBV)	ICA stenosis or occlusion	20	Feasibility study demonstrating that CBV-weighted reactivity is altered in patients relative to control subjects
71	Van Laar*	2008	ASL (CBF)	ICA stenosis or occlusion	130	Hypertension is related to higher CBF and hyperhomocysteinemia to lower regional CBF
72	Chng	2008	ASL (CBF)	ECA or ICA stenosis	18	Agreement observed between digital subtraction angiography and territorial ASL for the assessment of collateral flow
73	Haller*	2008	BOLD (CBF, CBV, $CMRO_2$)	ICA stenosis	24	Severely reduced pretreatment CO_2-induced BOLD reactivity was associated with increased occurrence of peri-interventional therapy infarction
74	Mandell	2008	BOLD (CBF, CBV) and ASL (CBF)	ICA stenosis	38	CO_2-induced BOLD reactivity correlates with CO_2-induced CBF-weighted ASL reactivity
75	Van Laar*	2007	ASL (CBF)	ICA stenosis	24	Differences in flow territories and regional CBF between patients and control subjects reduced after carotid angioplasty with stent placement; changes in flow territories and regional CBF were similar in patients who underwent carotid angioplasty with stent placement or carotid endarterectomy
76	Van Laar	2007	ASL (CBF)	ICA occlusion	68	Vessel-selective ASL maps show significant differences in flow territories of the contralateral ICA and vertebrobasilar arteries in patients compared with control subjects
77	Hendrikse	2005	ASL (CBF)	ICA sacrifice	7	Feasibility established for ASL for clinical follow-up of patients after extracranial-intracranial bypass surgery
78	Ziyeh*	2005	BOLD (CBF, CBV, $CMRO_2$)	ICA stenosis or occlusion	27	BOLD reactivity measurements include diagnostic information concerning cerebrovascular reserve
79	Hendrikse*	2004	ASL (CBF)	ICA occlusion	11	Reduced CBF in gray matter of hemisphere ipsilateral to occlusion compared with contralateral hemisphere
80	Ances	2004	ASL (CBF)	ICA stenosis	10	Inverse relationship found between change in CBF after carotid endarterectomy versus baseline CBF within the anterior circulation but not for posterior circulation
81	Detre	1999	ASL (CBF)	ICA and/or middle cerebral artery stenosis	14	Feasibility study demonstrating ability of ASL to identify different patterns of CBF augmentation

(*Continued*)

Table 2. Continued

Citation	First Author	Year	MRI Technique (Parameter)	Disease	n	Findings
Cerebrovascular risk factors						
82	Hajjar*	2010	ASL (CBF)	Hypertension	62	Decrease in CO_2-induced CBF reactivity in hypertensive patients without stroke was comparable to the decrease in CBF reactivity in stroke patients without hypertension
83	Fierstra	2010	BOLD (CBF, CBV, $CMRO_2$)	Vascular steal phenomena	17	Spatial correspondence exists between vascular steal and cortical thinning
84	Hajjar*	2010	ASL (CBF)	Acute stroke	80	Nocturnal dipping of lesser magnitude in systolic and pulse pressure is associated with brain atrophy and worse functional status
85	Pollock*	2009	ASL (CBF)	Hospitalized patients with hypercapnic cerebral hyperperfusion or hypocapnic hypoperfusion	45	Significant positive linear relationship between ASL CBF and partial pressure of CO_2
86	Zaharchuk*	2009	ASL (CBF)	Cerebrovascular disease	139	Approximately half of patients with normal contrast-enhanced CBF imaging have abnormal ASL findings, suggesting ASL provides additional information
87	Wu*	2008	Vessel-encoded ASL (CBF)	ICA and/or middle cerebral artery stenosis	56	ASL detects the presence and origin of collateral flow
88	Van Laar*	2008	ASL (CBF)	Vascular risk factors	121	Increasing levels of tumor necrosis factor-α is significantly associated with higher regional CBF
Intracranial stenosis						
89	Mandell*	2011	BOLD (CBF, CBV, $CMRO_2$)	Intracranial stenosis with EC/IC bypass	25	Preoperative measurement of CO_2-induced BOLD reactivity predicts the hemodynamic effect of extracranial-intracranial bypass
90	Zaharchuk*	2011	ASL (CBF)	Moyamoya	18	ASL predicts the presence and intensity of collateral flow in patients
91	Heyn	2010	BOLD (CBF, CBV, $CMRO_2$)	Moyamoya	11	BOLD CO_2-induced reactivity correlates with modified Suzuki score
Sickle cell disease						
92	O'Gorman	2010	ASL (CBF)	Sickle cell disease	1	ASL demonstrates crossed-cerebellar diaschisis
93	Helton	2009	ASL (CBF)	Sickle cell disease	21	Hydroxyurea may normalize gray matter CBF but not white matter CBF in sickle cell anemia children
94	Van den Tweel	2009	ASL (CBF)	Sickle cell disease	12	No CBF difference observed between sickle cell patients and control subjects, yet more CBF asymmetry observed in patients
95	Oguz*	2003	ASL (CBF)	Sickle cell disease	14	Regional CBF variations observed in normal-appearing regions of structural MRI

ASL indicates arterial spin labeling; CBF, cerebral blood flow; AAT, arterial arrival time; TIA, transient ischemic attack; DWI, diffusion-weighted imaging; ICA, internal carotid artery; BOLD, blood oxygenation level–dependent MRI; CBV, cerebral blood volume; $CMRO_2$, cerebral metabolic rate of oxygen; iVASO, inflow vascular-space-occupancy.

*Selected studies with clinical implications, expanded in online-only Data Supplement Table 1 (http://stroke.ahajournals.org).

crystalline iron oxide nanoparticle (MION)–CBV,[106] PET CBV[21] 및 Gd-DSC[22]를 통한 타당성 검사가 확립되어 있어 VASO의 CBV에 대한 민감도를 강화시키고 있다. VASO는 신경혈관커플링,[108] 기능적 MRI 방법론[109–112]과 함께 협착-폐색질환[22,70] 알츠하이머병[113] 및 암[114,115]에 대한 임상적 적용과 같은 다양한 범위에 적용되고 있다.

최근 VASO 연쇄의 변경이 도입되어 영상 용적 아래의 혈액내 물만을 영점화할 수 있게 되었다. 이러한 유입 VASO (inflow VASO, iVASO) 접근법으로 통상적인 VASO에 비해 신호대 잡음비를 증가시켜 동맥 CBV (aCBV)의 변화를 원칙적으로 민감하게 측정할 수 있게 되었다.[116] iVASO의 추가적인 발전으로 들 수 있는 iVASO 역동감쇄(iVASO with dynamic subtraction, iVASO-DS)는 일련으로 얻어진 대조군(조직+혈액 신호)과 영점군(조직 신호) 영상 사이의 차이를 이용하여 절대적 aCBV를 정량화할 수 있다.[22] 감산 절차는 ASL과 유사한데 ASL에서는 혈액내 물이 표식부탁되는 데 반해 iVASO-DS에서는 혈액내 물신호가 혈액내 물의 영점시간(혈액 영점화에 필요한 시간은 700~1100 ms 정도의 동맥-모세혈관 이행시간과 비슷하므로 왜 이러한 값이 동맥 의존적인지 알 수 있다)에 반응하는 표지지연을 선택함으로써 영점화되는 차이를 보인다.

iVASO-DS를 이용한 aCBV의 값은 문헌보고에서 기대한 값과 일치하게 보고되고 있으며 대상자 간 aCBV 값의 차이는 생리적으로 예상되는 범위를 넘어 다양하다. 어떠한 영상 방법이 이용되고 어떠한 부위가 연구되는지에 따라 총 회색질 CBV는 일반적으로 4.7~5.5 mL/100 mL으로 보고되며,[117] 정상인의 모세혈관 전 CBV는 전체 CBV의 20~30% 정도로 근사계

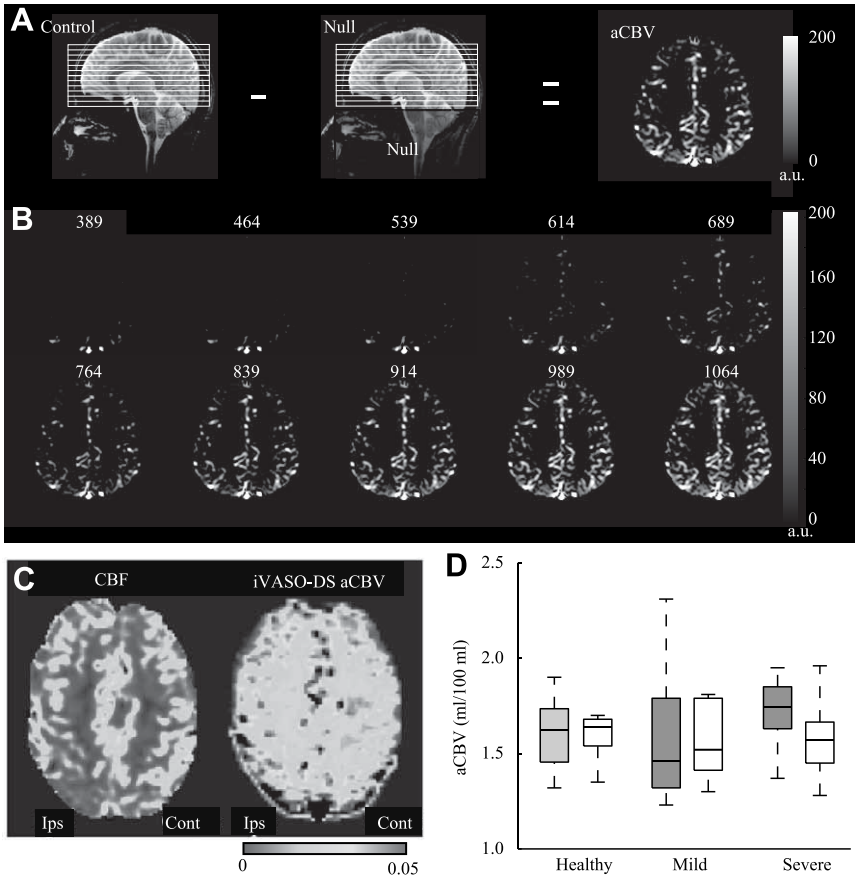

Figure 3. Noninvasive arterial cerebral blood volume (aCBV)-weighted vascular-space-occupancy with dynamic subtraction–dynamic subtraction (iVASO-DS) MRI. **A**, In iVASO-DS, the difference between images with and without inflowing blood water signal yields an aCBV-weighted map. **B**, Such images can be acquired at different labeling delays while keeping the blood water nulled in the null acquisitions, thereby yielding maps of inflowing microvascular aCBV as a function of time (ms; **above**). **C**, Axial slices from a patient with 70% right internal carotid artery (ICA) stenosis. **Left**, CBF-weighted slice from gadolinium–dynamic susceptibility contrast, and **right**, iVASO-DS aCBV map. CBF is symmetrical, yet aCBV is increased in the right parietal lobe, consistent with autoregulation. **D**, Box plots from patients (n=17) with varying degrees of ICA stenosis (mild, 15%≤ICA stenosis <70%; severe, ≥70% ICA stenosis). aCBV was asymmetrically elevated in 41% of patients studied (dark gray is ipsilateral to maximum stenosis).

산 된다.[118] 이러한 값에서 예상되는 aCBV는 0.94~1.65 mL/100 mL로 iVASO-DS aCBV 측정과 일치되는 결과이다. iVASO-DS는 최근 내경동맥 협착-폐색질환(Figure 3) 환자에서 CBV 변동을 평가하는 데 적용되고 있으며 Gd-DSC와의 비교[22]도 이루어지고 있다.

절대 aCBV의 평가를 위해 제안된 유사한 방법으로 동맥 지역 정량적 STAR 표지(quantitative STAR labeling of arterial regions, QUASAR)가 있다.[100] iVASO-DS와 유사하게 혈액내 물 신호를 가지고 있는 것과 가지고 있지 않는 데이터를 통한 감산으로 QUASAR에서의 aCBV에 대한 정량화가 이루어진다. 그러나 QUASAR에서 가로 혈액내 물 자기화는 양극성 탈위상기울기로 영점화되는데 비해 iVASO에서는 세로 혈액내 물 자기화는 역전회복의 원칙을 통하여 영점화된다. QUASAR은 대규모, 기관간 타당도 연구[45]가 진행되고 있으며 내경동맥 협착환자에서 SPECT와 비교할 만한 대비를 제공하는 것으로 보여지고 있다.[48]

CBV를 측정하는 다른 연구들이 제안되고 있으나 인체에서의 타당도 및 실현가능 정도는 아직 미흡하다. 9.4T에서 isoflurane 마취를 시행한 쥐에게 MOdulation of TIssue and VEssel (MOTIVE) 신호를 이용한 MRI 연구가 시행되었는데, 대뇌 피질의 aCBV는 1.1±0.5 mL/100 mL로 계산되었다.[101] MOTIVE 기법은 자화전달 및 ASL 기법을 이용하여 조직과 혈액내 물을 각각 구분하여 조정할 수 있다. 또한 용적추정에 대한 정맥재초점조정(venous refocusing for volume estimation, VERVE)법이 다양한 간격의 재초점 펄스를 통한 영상처리법[119]과 함께 정맥의 CBV 변화를 평가하는 비침습적인 방법으로 제안되었다. MOTIVE와 VERVE는 생리적인 CBV의 변화를 제공해주고 있으나 아직 임상적 환자에서 체계적으로 평가되지는 않았다.

산소 대사 및 소비

OEF와 $CMRO_2$는 혈류역학적 및 대사적 장애 정도를 평가할 수 있는 중요한 지표 중 하나이다. 뇌에서 CBF와 $CMRO_2$의 큰 변이가 있음에도 불구하고 OEF는 정상인에서 비교적 일정하게 유지된다. 이것은 초기의 혈류역학적 장애 시에도 적용되는데 이 당시에는 CBF및 CBV의 국소적 조절을 통해 OEF는 유지된다.[1] 급성기 뇌졸중에서 역치 아래로 감소한 CBF와 $CMRO_2$는 일반적으로 비가역적인 손상을 뜻한다. 그러나 CBF가 감소되어 있고 OEF가 증가되어 있는 동시에 $CMRO_2$가 보존되어 있는 비참한 관류(misery perfusion)는 아직 살아있는 조직을 뜻한다.

CBF와 마찬가지로 OEF의 측정은 $H_2{}^{15}O$를 이용한 PET의 사용으로 측정이 가능하게 되었다. OEF 측정과 유사한 MRI 접근법에 대한 노력이 이루어지고 있으나 이러한 방법들은 아

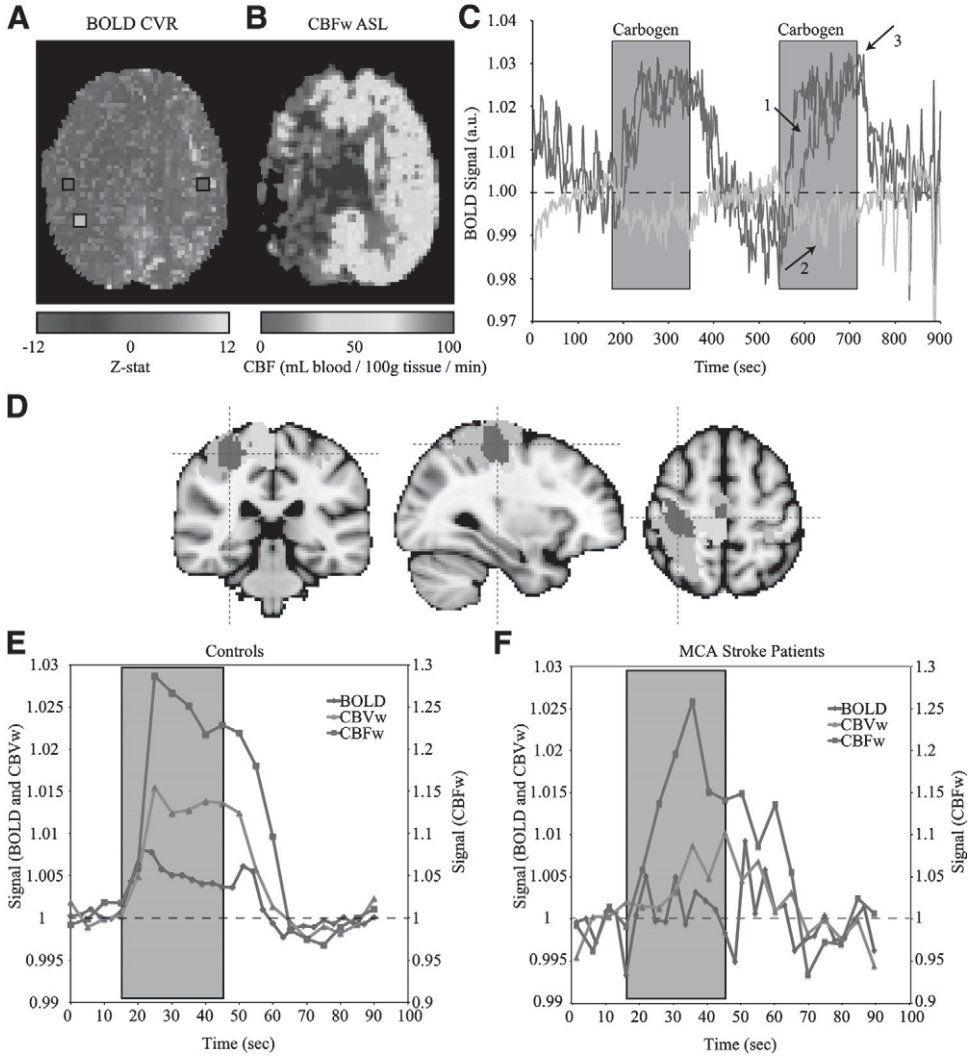

Figure 4. MRI reactivity in cerebrovascular disease. **A**, Moyamoya patient with decreased blood oxygenation level–dependent (BOLD) cerebrovascular reactivity (CVR) in right parietal lobe, and **B**, larger region of compromised cerebral blood flow (CBF) in the right hemisphere on arterial spin labeling (ASL). **C**, BOLD CVR time courses from colored voxels in **A** reveal heterogeneous response to carbogen administration (gray). This includes normal CVR and baseline CBF in the posterior left frontal lobe (blue), delayed CVR with delayed time-to-peak in the right frontal lobe (red; **arrows 1 and 3**), and even negative CVR (green; **arrow 2**), indicative of vascular steal phenomenon in the right parietal lobe. **D** through **F**, Hemodynamic time courses from chronic middle cerebral artery (MCA) stroke patients and controls acquired using BOLD, CBF-weighted ASL, and CBV-weighted vascular-space-occupancy fMRI in sequence. Patients (n=9) with enduring motor impairment were scanned within 1 year after stroke, at which time they performed unilateral joystick movement (f=1 Hz) with their affected hand. **D**, Activation maps (green), anatomic M1 (blue), and common regions (red) for all subjects, normalized to standard space. Time courses in common regions (**D**, red) show robust hemodynamic responses (gray box denotes stimulus period) in control subjects (n=11) but discord in CBF and CBV coupling in patients, eliciting absent ensemble patient BOLD reactivity.

직 개발단계에 있다. 명확한 시작단계는 blood oxygenation level dependent (BOLD) MRI로 이것은 뇌 기능을 평가하는 가장 일반적인 방법으로 떠오르게 되었다.[120] 간략히 말하면 BOLD 대비는 모세혈관과 정맥혈내의 산소수준이 증가하며 이에 따라 $T_2^{(*)}$연장(BOLD 효과)시키는 신경 혹은 혈관 활성[118]으로 인하여 CBV와 CMRO2에 대비한 CBF의 불균형적인 증가로 인해 발생한다. BOLD MRI는 다양하게 이용되고 있어 상당히 고공간(3~4 mm isotropic voxel dimensions)과 고시계열(2~3초)의 해상력을 가지고 쉽게 적용될 수 있다. 또한 가장 많이 시행되고 있는 BOLD 아형은 기본적으로 표준기울기에코연쇄(standard gradient echo sequence)를 사용하여 어떠한 MRI 장치에서도 이용 가능하다.

불행히도 BOLD 효과는 단지 신경활성의 간접적인 표지자이기 때문에 CBF, CBV, $CMRO_2$ 및 OEF에 대한 정량적 반응측정에 대한 연관이 활발히 연구되는 분야이다. 이러한 노력의 대부분은 신경 혹은 혈관 자극과 동시에 발생하는 CBF, CBV 및 OEF의 변화에 대한 연구로 집중되고 있다[18](Figure 4). 임상적으로 이러한 접근법은 만성 뇌혈관질환을 가진 환자에서 기대에 부응하는 정성적 결과를 제공하고 있으나[74,91] 아직 장애로 인해 임무에 대한 순응도가 떨어짐으로 인해서 급성기 환경

에서는 폭넓게 적용되고 있지는 않다. 따라서 최근의 연구들은 기초 영상으로부터 OEF를 정량적으로 추출하는 데 초점을 맞추고 있다. OEF를 정량화하기 위해 기초 BOLD 신호에 적용 가능한 모델을 이용한 실현가능성이 증명되고 있다. 이는 2000년도에 제시되어 2007년에 좀 더 섬세한 다중분획모델로의 적용이 다시 논의되고 있다.[121,122] 이러한 방법은 정상 자원자에서 생리적인 OEF값을 제공하고 있으며, 급성기 뇌졸중 환자에서 허혈성 뇌경색 부위 주변의 OEF를 특징짓는 데 사용되었으나[123] 아직은 섬세한 모델화 및 정량화 가정에 대한 어려움이 있어 임상적으로 큰 주목을 받지는 못하고 있다.

더욱 최근에 T_2-relaxation-under-spintagging (TRUST)라 불리는 전체 뇌의 OEF를 측정할 수 있는 방법이 제안되었다.[124] 이 방법은 정맥의 T_2를 시상정맥굴에서 측정한 이후 혈액 내 물의 T_2와 산소수준과의 알려진 관계에 기초하여 산소화수준의 할당이 이루어진다. 이 방법은 전체 뇌의 OEF를 측정할 수 있고 대상자 간 BOLD variation의 변이를 설명할 수 있는 잠재력을 가지고 있으나[125] OEF의 국소 변이를 측정할 수는 없는 단점도 있다. 정맥 혈액 표지와 속도 선택 ASL 원리를 이용하여 정맥 산소화를 좀 더 국소화시키는 방법으로 TRUST의 새로운 발전이 제시되고 있다. 이 방법은[126] OEF의 국소변이에 더욱 민감하기는 하나 임상 실현가능성 및 검사 간 타당성 연구는 아직 수행되지 않고 있다.

임상적 실현가능성 및 결론

저자들은 뇌혈관질환에서 CBF, CBV, $CMRO_2$ 및 OEF를 측정할 수 있는 새로운 MRI법에 대해 요약하였다. 이러한 접근법을 사용한 연구들은 대부분 만성 뇌혈관질환을 대상으로 한 연구들로 급성기 뇌졸중 영상에 대해서는 아직 초점이 맞춰져 있지는 않다. 주된 이유는 스캔에 시간이 필요하고(한 방법당 약 5분 정도), 영상 처리를 위해 필요한 시간이 급성기 시간 수요에는 일반적으로 최적화되어 있지 않기 때문이다. 그러나 이러한 방법들이 점점 표준화되면서 효율적이고 신속한 처리 방법에 대한 수요가 늘고 분석패키지가 시간에 민감한 영상들을 수월하게 스캐너 계기판으로 전달해줄 것으로 기대된다. 일반적으로 CBF가중 ASL 방법은 가장 진보된 임상적 시험을 겪고 있으며 Gd-DSC, PET 및 SPECT와의 상호타당성이 연구되고 있고(Table 1), 가장 광범위하게 뇌혈관질환에 적용되고 있다(Table 2). pCASL법은 MRI 스캐너에서 다양하게 적용 가능한 표준 하드웨어를 이용하여 5분 미만의 시간과 3~4 mm 등방성 혹은 전체 뇌 커버리지의 해상력을 통하여 Gd-DSC를 합리적으로 대체 적용할 수 있게 되었다. 1.5~2초의 표지후지연이 일반적으로 사용되나 AAT가 늘어난 뇌허혈환자에게는 더욱 긴 지연시간 혹은 다중 지연시간 프로토콜(5~8분)이 요구된다. PET, SPECT 및 Gd-DSC와 같은 다른 방법들과는 차별적으로 ASL법은 각각의 다른 혈관에 있는 혈액내 물을 표지할 수 있도록 변형될 수 있어 CBF에 대한 영상뿐만이 아니라 곁순환(예, 다른 영양 혈관으로부터 공급받는 CBF의 양어 어떠한지)에 대한 영상도 얻을 수 있다. 비침습적 CBV 측정법들은 CBF 적용법에 비해 덜 발달되어 있어 VASO와 QUASAR만이 인체 만성 뇌혈관질환 연구에 적용되고 있다. 이러한 방법들은 비정상 CBF와 CBV 커플링을 보이는 환자들에서 유용할 수 있는데, ASL법을 접목할 경우 곁순환과 자동조절에 대한 정량적인 정보도 제공할 수 있다. OEF와 $CMRO_2$를 측정할 수 있는 MRI법은 아직 개발 중으로 여러 방법들이 기대되고 있으나 아직 임상적 적용은 극히 제한적이다. 온라인으로만 제공되는 부록 Table 1에 이러한 방법들에 대한 연구들의 임상적 타당성이 자세하게 제시되어 있다.

Sources of Funding

Dr Hendrikse receives support from The Netherlands Heart Foundation (grant-2010B274).

Disclosures

None.

References

1. Derdeyn CP, Videen TO, Yundt KD, Fritsch SM, Carpenter DA, Grubb RL, et al. Variability of cerebral blood volume and oxygen extraction: stages of cerebral haemodynamic impairment revisited. *Brain*. 2002; 125:595–607.
2. Zipfel GJ, Sagar J, Miller JP, Videen TO, Grubb RL Jr, Dacey RG Jr, et al. Cerebral hemodynamics as a predictor of stroke in adult patients with Moyamoya disease: a prospective observational study. *Neurosurg Focus*. 2009;26:E6.
3. Grubb RL Jr, Derdeyn CP, Fritsch SM, Carpenter DA, Yundt KD, Videen TO, et al. Importance of hemodynamic factors in the prognosis of symptomatic carotid occlusion. *JAMA*. 1998;280: 1055–1060.
4. Gonzalez RG, Schaefer PW, Buonanno FS, Schwamm LH, Budzik RF, Rordorf G, et al. Diffusion-weighted MR imaging: diagnostic accuracy in patients imaged within 6 hours of stroke symptom onset. *Radiology*. 1999;210:155–162.
5. Wintermark M, Albers GW, Alexandrov AV, Alger JR, Bammer R, Baron JC, et al. Acute stroke imaging research roadmap. *Stroke*. 2008; 39:1621–1628.
6. Muir KW, Buchan A, von Kummer R, Rother J, Baron JC. Imaging of acute stroke. *Lancet Neurol*. 2006;5:755–768.
7. Hacke W, Albers G, Al-Rawi Y, Bogousslavsky J, Davalos A, Eliasziw M, et al. The desmoteplase in acute ischemic stroke trial (DIAS): a phase II MRI-based 9-hour window acute stroke thrombolysis trial with intravenous desmoteplase. *Stroke*. 2005;36:66–73.
8. Hacke W, Furlan AJ, Al-Rawi Y, Davalos A, Fiebach JB, Gruber F, et al. Intravenous desmoteplase in patients with acute ischaemic stroke selected by MRI perfusion-diffusion weighted imaging or perfusion ct (DIAS-2): a prospective, randomised, double-blind, placebo-controlled study. *Lancet Neurol*. 2009;8:141–150.
9. Furlan AJ, Eyding D, Albers GW, Al-Rawi Y, Lees KR, Rowley HA, et al. Dose escalation of desmoteplase for acute ischemic stroke (DEDAS): evidence of safety and efficacy 3 to 9 hours after stroke onset. *Stroke*. 2006;37:1227–1231.
10. Albers GW, Thijs VN, Wechsler L, Kemp S, Schlaug G, Skalabrin E, et al. Magnetic resonance imaging profiles predict clinical response to early reperfusion: the diffusion and perfusion imaging evaluation for understanding stroke evolution (DEFUSE) study. *Ann Neurol*. 2006;60: 508–517.
11. Lansberg MG, Lee J, Christensen S, Straka M, De Silva DA, Mlynash M, et al. Rapid automated patient selection for reperfusion therapy: a pooled analysis of the echoplanar imaging thrombolytic evaluation trial

(EPITHET) and the diffusion and perfusion imaging evaluation for understanding stroke evolution (DEFUSE) study. *Stroke*. 2011;42: 1608–1614.
12. Galinovic I, Ostwaldt AC, Soemmer C, Bros H, Hotter B, Brunecker P, et al. Search for a map and threshold in perfusion MRI to accurately predict tissue fate: a protocol for assessing lesion growth in patients with persistent vessel occlusion. *Cerebrovascular diseases*. 2011;32: 186–193.
13. Jalandhara N, Arora R, Batuman V. Nephrogenic systemic fibrosis and gadolinium-containing radiological contrast agents: an update. *Clin Pharmacol Ther*. 2011;89:920–923.
14. Williams DS, Detre JA, Leigh JS, Koretsky AP. Magnetic resonance imaging of perfusion using spin inversion of arterial water. *Proc Natl Acad Sci U S A*. 1992;89:212–216.
15. Buxton RB, Frank LR, Wong EC, Siewert B, Warach S, Edelman RR. A general kinetic model for quantitative perfusion imaging with arterial spin labeling. *Magn Reson Med*. 1998;40:383–396.
16. Raichle ME. Measurement of local cerebral blood flow and metabolism in man with positron emission tomography. *Fed Proc*. 1981;40: 2331–2334.
17. Rooney WD, Johnson G, Li X, Cohen ER, Kim SG, Ugurbil K, et al. Magnetic field and tissue dependencies of human brain longitudinal 1H2O relaxation in vivo. *Magn Reson Med*. 2007;57:308–318.
18. Donahue MJ, Blicher JU, Ostergaard L, Feinberg DA, MacIntosh BJ, Miller KL, et al. Cerebral blood flow, blood volume, and oxygen metabolism dynamics in human visual and motor cortex as measured by whole-brain multi-modal magnetic resonance imaging. *J Cereb Blood Flow Metab*. 2009;29:1856–1866.
19. Noguchi T, Kawashima M, Irie H, Ootsuka T, Nishihara M, Matsushima T, et al. Arterial spin-labeling MR imaging in Moyamoya disease compared with SPECT imaging. *Eur J Radiol*. 2011;80:e557–e562.
20. Liu P, Aslan S, Li X, Buhner DM, Spence JS, Briggs RW, et al. Perfusion deficit to cholinergic challenge in veterans with Gulf War illness. *Neurotoxicology*. 2011;32:242–246.
21. Uh J, Lin AL, Lee K, Liu P, Fox P, Lu H. Validation of VASO cerebral blood volume measurement with positron emission tomography. *Magn Reson Med*. 2011;65:744–749.
22. Donahue MJ, Sideso E, MacIntosh BJ, Kennedy J, Handa A, Jezzard P. Absolute arterial cerebral blood volume quantification using inflow vascular-space-occupancy with dynamic subtraction magnetic resonance imaging. *J Cereb Blood Flow Metab*. 2010;30:1329–1342.
23. Wissmeyer M, Altrichter S, Pereira VM, Viallon M, Federspiel A, Seeck M, et al. Arterial spin-labeling MRI perfusion in tuberous sclerosis: correlation with PET. *J Neuroradiol*. 2010;37:127–130.
24. Xu G, Rowley HA, Wu G, Alsop DC, Shankaranarayanan A, Dowling M, et al. Reliability and precision of pseudo-continuous arterial spin labeling perfusion MRI on 3.0 T and comparison with 15O-water pet in elderly subjects at risk for Alzheimer's disease. *NMR Biomed*. 2010;23: 286–293.
25. Qiu M, Paul Maguire R, Arora J, Planeta-Wilson B, Weinzimmer D, Wang J, et al. Arterial transit time effects in pulsed arterial spin labeling CBF mapping: insight from a PET and MR study in normal human subjects. *Magn Reson Med*. 2010;63:374–384.
26. Bokkers RP, Bremmer JP, van Berckel BN, Lammertsma AA, Hendrikse J, Pluim JP, et al. Arterial spin labeling perfusion MRI at multiple delay times: a correlative study with H(2)(15)O positron emission tomography in patients with symptomatic carotid artery occlusion. *J Cereb Blood Flow Metab*. 2010;30:222–229.
27. Knutsson L, van Westen D, Petersen ET, Bloch KM, Holtas S, Stahlberg F, et al. Absolute quantification of cerebral blood flow: correlation between dynamic susceptibility contrast MRI and model-free arterial spin labeling. *Magn Reson Imaging*. 2009;28:1–7.
28. Ludemann L, Warmuth C, Plotkin M, Forschler A, Gutberlet M, Wust P, et al. Brain tumor perfusion: comparison of dynamic contrast enhanced magnetic resonance imaging using T1, T2, and T2* contrast, pulsed arterial spin labeling, and H2(15)O positron emission tomography. *Eur J Radiol*. 2009;70:465–474.
29. Chen JJ, Wieckowska M, Meyer E, Pike GB. Cerebral blood flow measurement using fMRI and PET: a cross-validation study. *Int J Biomed Imaging*. 2008;2008:516359.
30. Newberg AB, Wang J, Rao H, Swanson RL, Wintering N, Karp JS, et al. Concurrent CBF and CMRGLC changes during human brain activation by combined fMRI-pet scanning. *Neuroimage*. 2005;28: 500–506.
31. Kimura H, Kado H, Koshimoto Y, Tsuchida T, Yonekura Y, Itoh H. Multislice continuous arterial spin-labeled perfusion MRI in patients with chronic occlusive cerebrovascular disease: a correlative study with CO_2 PET validation. *J Magn Reson Imaging*. 2005;22:189–198.
32. Wintermark M, Sesay M, Barbier E, Borbely K, Dillon WP, Eastwood JD, et al. Comparative overview of brain perfusion imaging techniques. *J Neuroradiol*. 2005;32:294–314.
33. Weber MA, Gunther M, Lichy MP, Delorme S, Bongers A, Thilmann C, et al. Comparison of arterial spin-labeling techniques and dynamic susceptibility-weighted contrast-enhanced MRI in perfusion imaging of normal brain tissue. *Invest Radiol*. 2003;38:712–718.
34. Liu HL, Kochunov P, Hou J, Pu Y, Mahankali S, Feng CM, et al. Perfusion-weighted imaging of interictal hypoperfusion in temporal lobe epilepsy using fair-haste: comparison with H(2)(15)O PET measurements. *Magn Reson Med*. 2001;45:431–435.
35. Ye FQ, Berman KF, Ellmore T, Esposito G, van Horn JD, Yang Y, et al. H(2)(15)O PET validation of steady-state arterial spin tagging cerebral blood flow measurements in humans. *Magn Reson Med*. 2000;44: 450–456.
36. Golay X, Hendrikse J, Lim TC. Perfusion imaging using arterial spin labeling. *Top Magn Reson Imaging*. 2004;15:10–27.
37. Kim SG. Quantification of relative cerebral blood flow change by flow-sensitive alternating inversion recovery (fair) technique: application to functional mapping. *Magn Reson Med*. 1995;34: 293–301.
38. Golay X, Stuber M, Pruessmann KP, Meier D, Boesiger P. Transfer insensitive labeling technique (TILT): application to multislice functional perfusion imaging. *J Magn Reson Imaging*. 1999;9: 454–461.
39. Wong EC, Buxton RB, Frank LR. A theoretical and experimental comparison of continuous and pulsed arterial spin labeling techniques for quantitative perfusion imaging. *Magn Reson Med*. 1998; 40:348–355.
40. Alsop DC, Detre JA. Multisection cerebral blood flow MR imaging with continuous arterial spin labeling. *Radiology*. 1998;208: 410–416.
41. Wu WC, Fernandez-Seara M, Detre JA, Wehrli FW, Wang J. A theoretical and experimental investigation of the tagging efficiency of pseudocontinuous arterial spin labeling. *Magn Reson Med*. 2007;58: 1020–1027.
42. Alsop DC, Connick TJ, Mizsei G. A spiral volume coil for improved RF field homogeneity at high static magnetic field strength. *Magn Reson Med*. 1998;40:49–54.
43. Gonzalez-At JB, Alsop DC, Detre JA. Cerebral perfusion and arterial transit time changes during task activation determined with continuous arterial spin labeling. *Magn Reson Med*. 2000;43:739–746.
44. MacIntosh BJ, Filippini N, Chappell MA, Woolrich MW, Mackay CE, Jezzard P. Assessment of arterial arrival times derived from multiple inversion time pulsed arterial spin labeling MRI. *Magn Reson Med*. 2010;63:641–647.
45. Petersen ET, Mouridsen K, Golay X. The quasar reproducibility study, part II: results from a multi-center arterial spin labeling test-retest study. *Neuroimage*. 2010;49:104–113.
46. MacIntosh BJ, Lindsay AC, Kylintireas I, Kuker W, Gunther M, Robson MD, et al. Multiple inflow pulsed arterial spin-labeling reveals delays in the arterial arrival time in minor stroke and transient ischemic attack. *Am J Neuroradiol*. 2010;31:1892–1894.
47. Bokkers RP, van der Worp HB, Mali WP, Hendrikse J. Noninvasive MR imaging of cerebral perfusion in patients with a carotid artery stenosis. *Neurology*. 2009;73:869–875.
48. Uchihashi Y, Hosoda K, Zimine I, Fujita A, Fujii M, Sugimura K, et al. Clinical application of arterial spin-labeling MR imaging in patients with carotid stenosis: quantitative comparative study with single-photon emission CT. *Am J Neuroradiol*. 2011 [Epub ahead of print].
49. van Osch MJ, Teeuwisse WM, van Walderveen MA, Hendrikse J, Kies DA, van Buchem MA. Can arterial spin labeling detect white matter perfusion signal? *Magn Reson Med*. 2009;62:165–173.
50. Wong EC, Cronin M, Wu WC, Inglis B, Frank LR, Liu TT. Velocity-selective arterial spin labeling. *Magn Reson Med*. 2006;55:1334–1341.
51. Hendrikse J, van der Grond J, Lu H, van Zijl PC, Golay X. Flow territory mapping of the cerebral arteries with regional perfusion MRI. *Stroke*. 2004;35:882–887.
52. Wong EC. Vessel-encoded arterial spin-labeling using pseudocontinuous tagging. *Magn Reson Med*. 2007;58:1086–1091.
53. Bokkers RP, van Osch MJ, Klijn CJ, Kappelle LJ, Hendrikse J. Cere-

brovascular reactivity within perfusion territories in patients with an internal carotid artery occlusion. *J Neurol Neurosurg Psychiatry*. 2011 [Epub ahead of print].
54. Garcia DM, Duhamel G, Alsop DC. Efficiency of inversion pulses for background suppressed arterial spin labeling. *Magn Reson Med*. 2005; 54:366–372.
55. Ye FQ, Frank JA, Weinberger DR, McLaughlin AC. Noise reduction in 3D perfusion imaging by attenuating the static signal in arterial spin tagging (ASSIST). *Magn Reson Med*. 2000;44:92–100.
56. Gunther M, Oshio K, Feinberg DA. Single-shot 3D imaging techniques improve arterial spin labeling perfusion measurements. *Magn Reson Med*. 2005;54:491–498.
57. Fernandez-Seara MA, Wang Z, Wang J, Rao HY, Guenther M, Feinberg DA, et al. Continuous arterial spin labeling perfusion measurements using single shot 3D Grase at 3 T. *Magn Reson Med*. 2005;54: 1241–1247.
58. Filippini N, MacIntosh BJ, Hough MG, Goodwin GM, Frisoni GB, Smith SM, et al. Distinct patterns of brain activity in young carriers of the apoE-epsilon4 allele. *Proc Natl Acad Sci U S A*. 2009;106: 7209–7214.
59. MacIntosh BJ, Pattinson KT, Gallichan D, Ahmad I, Miller KL, Feinberg DA, et al. Measuring the effects of remifentanil on cerebral blood flow and arterial arrival time using 3D Grase MRI with pulsed arterial spin labelling. *J Cereb Blood Flow Metab*. 2008;28: 1514–1522.
60. Chen J, Licht DJ, Smith SE, Agner SC, Mason S, Wang S, et al. Arterial spin labeling perfusion MRI in pediatric arterial ischemic stroke: initial experiences. *J Magn Reson Imaging*. 2009;29:282–290.
61. Hendrikse J, Petersen ET, Cheze A, Chng SM, Venketasubramanian N, Golay X. Relation between cerebral perfusion territories and location of cerebral infarcts. *Stroke*. 2009;40:1617–1622.
62. Zhao P, Alsop DC, Abduljalil A, Selim M, Lipsitz L, Novak P, et al. Vasoreactivity and peri-infarct hyperintensities in stroke. *Neurology*. 2009;72:643–649.
63. Pollock JM, Whitlow CT, Deibler AR, Tan H, Burdette JH, Kraft RA, et al. Anoxic injury-associated cerebral hyperperfusion identified with arterial spin-labeled MR imaging. *Am J Neuroradiol*. 2008;29: 1302–1307.
64. Wolf RL, Alsop DC, McGarvey ML, Maldjian JA, Wang J, Detre JA. Susceptibility contrast and arterial spin labeled perfusion MRI in cerebrovascular disease. *J Neuroimaging*. 2003;13:17–27.
65. Chalela JA, Alsop DC, Gonzalez-Atavales JB, Maldjian JA, Kasner SE, Detre JA. Magnetic resonance perfusion imaging in acute ischemic stroke using continuous arterial spin labeling. *Stroke*. 2000;31: 680–687.
66. Detre JA, Alsop DC, Vives LR, Maccotta L, Teener JW, Raps EC. Noninvasive MRI evaluation of cerebral blood flow in cerebrovascular disease. *Neurology*. 1998;50:633–641.
67. Bokkers RP, Wessels FJ, van der Worp HB, Zwanenburg JJ, Mali WP, Hendrikse J. Vasodilatory capacity of the cerebral vasculature in patients with carotid artery stenosis. *Am J Neuroradiol*. 2011;32: 1030–1033.
68. Hartkamp NS, Bokkers RP, van der Worp HB, van Osch MJ, Kappelle LJ, Hendrikse J. Distribution of cerebral blood flow in the caudate nucleus, lentiform nucleus and thalamus in patients with carotid artery stenosis. *Eur Radiol*. 2011;21:875–881.
69. Bokkers RP, van Osch MJ, van der Worp HB, de Borst GJ, Mali WP, Hendrikse J. Symptomatic carotid artery stenosis: impairment of cerebral autoregulation measured at the brain tissue level with arterial spin-labeling MR imaging. *Radiology*. 2010;256:201–208.
70. Donahue MJ, van Laar PJ, van Zijl PC, Stevens RD, Hendrikse J. Vascular space occupancy (VASO) cerebral blood volume-weighted MRI identifies hemodynamic impairment in patients with carotid artery disease. *J Magn Reson Imaging*. 2009;29:718–724.
71. van Laar PJ, van Raamt AF, van der Grond J, Mali WP, van der Graaf Y, Hendrikse J. Increasing levels of TNFalpha are associated with increased brain perfusion. *Atherosclerosis*. 2008;196:449–454.
72. Chng SM, Petersen ET, Zimine I, Sitoh YY, Lim CC, Golay X. Territorial arterial spin labeling in the assessment of collateral circulation: comparison with digital subtraction angiography. *Stroke*. 2008;39: 3248–3254.
73. Haller S, Bonati LH, Rick J, Klarhofer M, Speck O, Lyrer PA, et al. Reduced cerebrovascular reserve at Co_2 bold MR imaging is associated with increased risk of periinterventional ischemic lesions during carotid endarterectomy or stent placement: preliminary results. *Radiology*. 2008;249:251–258.
74. Mandell DM, Han JS, Poublanc J, Crawley AP, Stainsby JA, Fisher JA, et al. Mapping cerebrovascular reactivity using blood oxygen level-dependent MRI in patients with arterial steno-occlusive disease: comparison with arterial spin labeling MRI. *Stroke*. 2008;39: 2021–2028.
75. Van Laar PJ, Hendrikse J, Mali WP, Moll FL, van der Worp HB, van Osch MJ, et al. Altered flow territories after carotid stenting and carotid endarterectomy. *J Vasc Surg*. 2007;45:1155–1161.
76. van Laar PJ, Hendrikse J, Klijn CJ, Kappelle LJ, van Osch MJ, van der Grond J. Symptomatic carotid artery occlusion: flow territories of major brain-feeding arteries. *Radiology*. 2007;242:526–534.
77. Hendrikse J, van der Zwan A, Ramos LM, van Osch MJ, Golay X, Tulleken CA, et al. Altered flow territories after extracranial-intracranial bypass surgery. *Neurosurgery*. 2005;57:486–494.
78. Ziyeh S, Rick J, Reinhard M, Hetzel A, Mader I, Speck O. Blood oxygen level-dependent MRI of cerebral Co_2 reactivity in severe carotid stenosis and occlusion. *Stroke*. 2005;36:751–756.
79. Hendrikse J, van Osch MJ, Rutgers DR, Bakker CJ, Kappelle LJ, Golay X, et al. Internal carotid artery occlusion assessed at pulsed arterial spin-labeling perfusion MR imaging at multiple delay times. *Radiology*. 2004;233:899–904.
80. Ances BM, McGarvey ML, Abrahams JM, Maldjian JA, Alsop DC, Zager EL, et al. Continuous arterial spin labeled perfusion magnetic resonance imaging in patients before and after carotid endarterectomy. *J Neuroimaging*. 2004;14:133–138.
81. Detre JA, Samuels OB, Alsop DC, Gonzalez-At JB, Kasner SE, Raps EC. Noninvasive magnetic resonance imaging evaluation of cerebral blood flow with acetazolamide challenge in patients with cerebrovascular stenosis. *J Magn Reson Imaging*. 1999;10:870–875.
82. Hajjar I, Zhao P, Alsop D, Novak V. Hypertension and cerebral vasoreactivity: a continuous arterial spin labeling magnetic resonance imaging study. *Hypertension*. 2010;56:859–864.
83. Fierstra J, Poublanc J, Han JS, Silver F, Tymianski M, Crawley AP, et al. Steal physiology is spatially associated with cortical thinning. *J Neurol Neurosurg Psychiatry*. 2010;81:290–293.
84. Hajjar I, Zhao P, Alsop D, Abduljalil A, Selim M, Novak P, et al. Association of blood pressure elevation and nocturnal dipping with brain atrophy, perfusion and functional measures in stroke and nonstroke individuals. *Am J Hypertens*. 2010;23:17–23.
85. Pollock JM, Deibler AR, Whitlow CT, Tan H, Kraft RA, Burdette JH, et al. Hypercapnia-induced cerebral hyperperfusion: an underrecognized clinical entity. *Am J Neuroradiol*. 2009;30:378–385.
86. Zaharchuk G, Bammer R, Straka M, Shankaranarayan A, Alsop DC, Fischbein NJ, et al. Arterial spin-label imaging in patients with normal bolus perfusion-weighted MR imaging findings: pilot identification of the borderzone sign. *Radiology*. 2009;252:797–807.
87. Wu B, Wang X, Guo J, Xie S, Wong EC, Zhang J, et al. Collateral circulation imaging: MR perfusion territory arterial spin-labeling at 3T. *Am J Neuroradiol*. 2008;29:1855–1860.
88. van Laar PJ, van der Graaf Y, Mali WP, van der Grond J, Hendrikse J. Effect of cerebrovascular risk factors on regional cerebral blood flow. *Radiology*. 2008;246:198–204.
89. Mandell DM, Han JS, Poublanc J, Crawley AP, Fierstra J, Tymianski M, et al. Quantitative measurement of cerebrovascular reactivity by blood oxygen level-dependent MR imaging in patients with intracranial stenosis: preoperative cerebrovascular reactivity predicts the effect of extracranial-intracranial bypass surgery. *Am J Neuroradiol*. 2011;32: 721–727.
90. Zaharchuk G, Do HM, Marks MP, Rosenberg J, Moseley ME, Steinberg GK. Arterial spin-labeling MRI can identify the presence and intensity of collateral perfusion in patients with Moyamoya disease. *Stroke*. 2011 [Epub ahead of print].
91. Heyn C, Poublanc J, Crawley A, Mandell D, Han JS, Tymianski M, et al. Quantification of cerebrovascular reactivity by blood oxygen level-dependent MR imaging and correlation with conventional angiography in patients with Moyamoya disease. *Am J Neuroradiol*. 2010;31: 862–867.
92. O'Gorman RL, Siddiqui A, Alsop DC, Jarosz JM. Perfusion MRI demonstrates crossed-cerebellar diaschisis in sickle cell disease. *Pediatr Neurol*. 2010;42:437–440.
93. Helton KJ, Paydar A, Glass J, Weirich EM, Hankins J, Li CS, et al. Arterial spin-labeled perfusion combined with segmentation techniques to evaluate cerebral blood flow in white and gray matter of

children with sickle cell anemia. *Pediatr Blood Cancer*. 2009;52: 85–91.
94. van den Tweel XW, Nederveen AJ, Majoie CB, van der Lee JH, Wagener-Schimmel L, van Walderveen MA, et al. Cerebral blood flow measurement in children with sickle cell disease using continuous arterial spin labeling at 3.0-Tesla MRI. *Stroke*. 2009;40:795–800.
95. Oguz KK, Golay X, Pizzini FB, Freer CA, Winrow N, Ichord R, et al. Sickle cell disease: continuous arterial spin-labeling perfusion MR imaging in children. *Radiology*. 2003;227:567–574.
96. Villringer A, Rosen BR, Belliveau JW, Ackerman JL, Lauffer RB, Buxton RB, et al. Dynamic imaging with lanthanide chelates in normal brain: contrast due to magnetic susceptibility effects. *Magn Reson Med*. 1988;6:164–174.
97. Powers WJ, Raichle ME. Positron emission tomography and its application to the study of cerebrovascular disease in man. *Stroke*. 1985;16: 361–376.
98. Steiger HJ, Aaslid R, Stooss R. Dynamic computed tomographic imaging of regional cerebral blood flow and blood volume: a clinical pilot study. *Stroke*. 1993;24:591–597.
99. Sakai F, Nakazawa K, Tazaki Y, Ishii K, Hino H, Igarashi H, et al. Regional cerebral blood volume and hematocrit measured in normal human volunteers by single-photon emission computed tomography. *J Cereb Blood Flow Metab*. 1985;5:207–213.
100. Petersen ET, Lim T, Golay X. Model-free arterial spin labeling quantification approach for perfusion MRI. *Magn Reson Med*. 2006;55: 219–232.
101. Kim T, Kim SG. Quantification of cerebral arterial blood volume and cerebral blood flow using MRI with modulation of tissue and vessel (MOTIVE) signals. *Magn Reson Med*. 2005;54:333–342.
102. Lu H, Golay X, Pekar JJ, Van Zijl PC. Functional magnetic resonance imaging based on changes in vascular space occupancy. *Magn Reson Med*. 2003;50:263–274.
103. Gu H, Lu H, Ye FQ, Stein EA, Yang Y. Noninvasive quantification of cerebral blood volume in humans during functional activation. *Neuroimage*. 2006;30:377–387.
104. Scouten A, Constable RT. Vaso-based calculations of CBV change: accounting for the dynamic CSF volume. *Magn Reson Med*. 2008;59: 308–315.
105. Donahue MJ, Lu H, Jones CK, Edden RA, Pekar JJ, van Zijl PC. Theoretical and experimental investigation of the VASO contrast mechanism. *Magn Reson Med*. 2006;56:1261–1273.
106. Jin T, Kim SG. Spatial dependence of CBV-FMRI: a comparison between VASO and contrast agent based methods. *Conf Proc IEEE Eng Med Biol Soc*. 2006;1:25–28.
107. Donahue MJ, Hua J, Pekar JJ, van Zijl PC. Effect of inflow of fresh blood on vascular-space-occupancy (VASO) contrast. *Magn Reson Med*. 2009;61:473–480.
108. Donahue MJ, Stevens RD, de Boorder M, Pekar JJ, Hendrikse J, van Zijl PC. Hemodynamic changes after visual stimulation and breath holding provide evidence for an uncoupling of cerebral blood flow and volume from oxygen metabolism. *J Cereb Blood Flow Metab*. 2009;29: 176–185.
109. Wu CW, Liu HL, Chen JH, Yang Y. Effects of CBV, CBF, and blood-brain barrier permeability on accuracy of PASL and VASO measurement. *Magn Reson Med*. 2010;63:601–608.
110. Poser BA, Norris DG. Measurement of activation-related changes in cerebral blood volume: VASO with single-shot haste acquisition. *Magma*. 2007;20:63–67.
111. Hua J, Donahue MJ, Zhao JM, Grgac K, Huang AJ, Zhou J, et al. Magnetization transfer enhanced vascular-space-occupancy (MT-VASO) functional MRI. *Magn Reson Med*. 2009;61:944–951.
112. Poser BA, Norris DG. Application of whole-brain CBV-weighted fMRI to a cognitive stimulation paradigm: robust activation detection in a Stroop task experiment using 3D Grase VASO. *Hum Brain Mapp*. 2011;32:974–981.
113. Uh J, Lewis-Amezcua K, Martin-Cook K, Cheng Y, Weiner M, Diaz-Arrastia R, et al. Cerebral blood volume in Alzheimer's disease and correlation with tissue structural integrity. *Neurobiol Aging*. 2010;31: 2038–2046.
114. Donahue MJ, Blakeley JO, Zhou J, Pomper MG, Laterra J, van Zijl PC. Evaluation of human brain tumor heterogeneity using multiple T1-based MRI signal weighting approaches. *Magn Reson Med*. 2008; 59:336–344.
115. Lu H, Pollack E, Young R, Babb JS, Johnson G, Zagzag D, et al. Predicting grade of cerebral glioma using vascular-space occupancy MR imaging. *Am J Neuroradiol*. 2008;29:373–378.
116. Hua J, Qin Q, Donahue MJ, Zhou J, Pekar JJ, van Zijl PC. Inflow-based vascular-space-occupancy (IVASO) MRI. *Magn Reson Med*. 2011;66: 40–56.
117. Leenders KL, Perani D, Lammertsma AA, Heather JD, Buckingham P, Healy MJ, et al. Cerebral blood flow, blood volume and oxygen utilization: normal values and effect of age. *Brain*. 1990;113:27–47.
118. van Zijl PC, Eleff SM, Ulatowski JA, Oja JM, Ulug AM, Traystman RJ, et al. Quantitative assessment of blood flow, blood volume and blood oxygenation effects in functional magnetic resonance imaging. *Nat Med*. 1998;4:159–167.
119. Stefanovic B, Pike GB. Venous refocusing for volume estimation: Verve functional magnetic resonance imaging. *Magn Reson Med*. 2005;53: 339–347.
120. Ogawa S, Lee TM, Kay AR, Tank DW. Brain magnetic resonance imaging with contrast dependent on blood oxygenation. *Proc Natl Acad Sci U S A*. 1990;87:9868–9872.
121. An H, Lin W. Quantitative measurements of cerebral blood oxygen saturation using magnetic resonance imaging. *J Cereb Blood Flow Metab*. 2000;20:1225–1236.
122. He X, Yablonskiy DA. Quantitative BOLD: mapping of human cerebral deoxygenated blood volume and oxygen extraction fraction: default state. *Magn Reson Med*. 2007;57:115–126.
123. Lee JM, Vo KD, An H, Celik A, Lee Y, Hsu CY, et al. Magnetic resonance cerebral metabolic rate of oxygen utilization in hyperacute stroke patients. *Ann Neurol*. 2003;53:227–232.
124. Lu H, Ge Y. Quantitative evaluation of oxygenation in venous vessels using T2-relaxation-under-spin-tagging MRI. *Magn Reson Med*. 2008; 60:357–363.
125. Lu H, Zhao C, Ge Y, Lewis-Amezcua K. Baseline blood oxygenation modulates response amplitude: physiologic basis for intersubject variations in functional MRI signals. *Magn Reson Med*. 2008;60: 364–372.
126. Bolar DS, Rosen BR, Sorensen AG, Adalsteinsson E. Quantitative imaging of extraction of oxygen and tissue consumption (quixotic) using venular-targeted velocity-selective spin labeling. *Magn Reson Med*. 2011 [E-pub ahead of print].